FINAL TECHNICAL REPORT

ON

THE USE OF ELECTROCHEMISTRY AND ELLIPSOMETRY FOR IDENTIFYING AND EVALUATING CORROSION ON AIRCRAFT

SMALL BUSINESS INNOVATIVE RESEARCH (SBIR)
PROGRAM SOLICITATION 94-1
PHASE 1 - CONTROL NUMBER 94-NC-133

Submitted by

Chester M. Dacres
DACCO SCI, INC.
10260 Old Columbia Road
Suite A1
Columbia, MD 21046-1218

Submitted to

Major Thomas E. Erstfeld
Project Manager
Directorate of Chemistry and Material Science
Department of the Air Force
Air Force Office of Scientific Research (AFOSR)
110 Duncan Ave.
Bolling AFB, DC 20332-0001

15 June 1994 - 14 December 1994

1. AGENCY USE ONLY (Leave blank)	2. REPORT DATE	3. REPORT TYPE AND DATES COVERED
	15 Dec 94	Final Report 15 Jun - 15 Dec 94

4. TITLE AND SUBTITLE
The Use of Electrochemistry and Ellipsometry For Identifying and Evaluating Corrosion on Aircraft.

5. FUNDING NUMBERS
3005/SS
Program Solicitation 94-1
Control # 94-NC-133
Contract # F49620-94-C-0042

6. AUTHOR(S)
Chester M. Dacres & Brian C. Taggart (DACCO SCI, INC.)
Charles R. Anderson & Pam Whisnant (Martin Marietta Laboratories)

7. PERFORMING ORGANIZATION NAME(S) AND ADDRESS(ES)
DACCO SCI, INC.
10260 Old Columbia Road
Columbia, MD 21046

8. PERFORMING ORGANIZATION REPORT NUMBER
Final Report
AFOSR-TR- 95 0006

9. SPONSORING/MONITORING AGENCY NAME(S) AND ADDRESS(ES)
Air Force Office of Scientific Research (AFOSR)
110 Duncan Avenue
Bolling AFB, DC 20332-0001

10. SPONSORING/MONITORING AGENCY REPORT NUMBER

11. SUPPLEMENTARY NOTES
Performed in conjunction with Martin Marietta Laboratories - Baltimore

12a. DISTRIBUTION/AVAILABILITY STATEMENT
Unrestricted

12b. DISTRIBUTION CODE
A

13. ABSTRACT *(Maximum 200 words)*

Electrochemical corrosion testing using AC impedance measurement and ellipsometry has been performed on aircraft aluminum 2024-T3 samples. The AC Impedance technique was used to acquire a precise low-frequency impedance signature of corroding painted aircraft aluminum which will be used to develop a simple, yet powerful, sensor for the early detection and measurement of corrosion processes on aircraft. The use of ellipsometry and DC electrochemical techniques, have verified that the low-frequency impedance spectrum obtained from the AC Impedance technique is representative of the corrosion process for painted aircraft aluminum 2024-T3. Based on these findings, several versions of prototype electrode sensors were developed capable of obtaining this signature utilizing a two-electrode approach. These *in-situ* electrode sensors were extensively tested using AC Impedance, electrochemistry, ellipsometry, and X-ray Photoelectron Spectroscopy. Results indicate the ability of the electrode sensors to non-destructively monitor the corrosion process on aircraft aluminum 2024-T3 and to withstand harsh operating environments.

14. SUBJECT TERMS				15. NUMBER OF PAGES
Aircraft	Electrochemistry	AC Impedance	Electrode	75
Corrosion	XPS	Ellipsometry	Sensors	16. PRICE CODE

17. SECURITY CLASSIFICATION OF REPORT	18. SECURITY CLASSIFICATION OF THIS PAGE	19. SECURITY CLASSIFICATION OF ABSTRACT	20. LIMITATION OF ABSTRACT
Unclassified	Unclassified	Unclassified	UL

NSN 7540-01-280-5500

Standard Form 298 (Rev 2-89)
Prescribed by ANSI Std 239-18
298-102

DISCLAIMER NOTICE

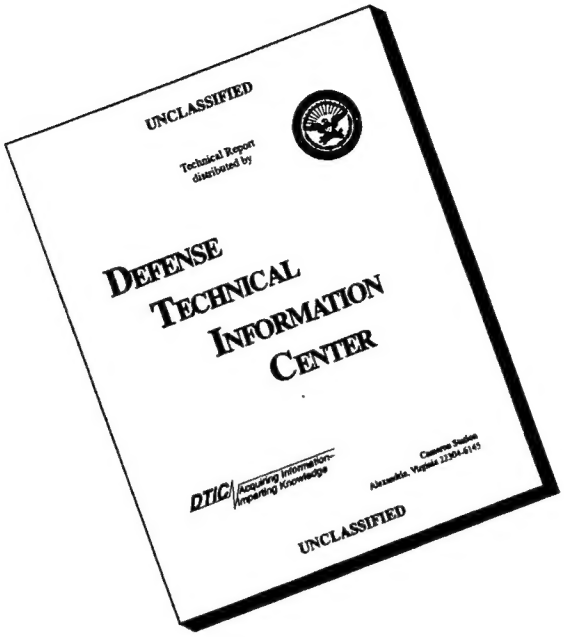

THIS DOCUMENT IS BEST QUALITY AVAILABLE. THE COPY FURNISHED TO DTIC CONTAINED A SIGNIFICANT NUMBER OF PAGES WHICH DO NOT REPRODUCE LEGIBLY.

FINAL TECHNICAL REPORT

ON

THE USE OF ELECTROCHEMISTRY AND ELLIPSOMETRY FOR IDENTIFYING AND EVALUATING CORROSION ON AIRCRAFT

SMALL BUSINESS INNOVATIVE RESEARCH (SBIR)
PROGRAM SOLICITATION 94-1
PHASE 1 - CONTROL NUMBER 94-NC-133

Submitted by

Chester M. Dacres
DACCO SCI, INC.
10260 Old Columbia Road
Suite A1
Columbia, MD 21046-1218

Submitted to

Major Thomas E. Erstfeld
Project Manager
Directorate of Chemistry and Material Science
Department of the Air Force
Air Force Office of Scientific Research (AFOSR)
110 Duncan Ave.
Bolling AFB, DC 20332-0001

15 June 1994 - 14 December 1994

DSI

DACCO SCI, INC.

CORROSION ENGINEERING-MATERIALS TECHNOLOGY-ELECTROCHEMISTRY

10260 OLD COLUMBIA ROAD. COLUMBIA. MD 21046
BALT. (410) 381-9475 • DC (301) 596-7019 • FAX (410) 381-9643

December 15, 1994

Major Thomas C. Erstfeld, USAF
Program Manager
Directorate of Chemistry and Material Science
Department of the Air Force
Air Force Office of Scientific Research (AFOSR)
110 Duncan Avenue
Bolling AFB, DC 20332-0001

Re: SBIR Phase 1 - Control No. 94-NC-133
The Use of Electrochemistry and Ellipsometry for Identifying and Evaluating Corrosion on Aircraft.

Dear Major Erstfeld

Enclosed please find a copy of the final technical report entitled "The Use of Electrochemistry and Ellipsometry for Identifying and Evaluating Corrosion on Aircraft."

Chester M. Dacres and Brian C. Taggart of DACCO SCI, INC. and Charles R. Anderson and Pamela Whisnant of Martin Marietta Laboratories • Baltimore contributed to this report.

Phase I has produced a feasibility that shows that, using AC Impedance, it is possible to recognize a distinct degradation pattern for aircraft material. In-situ electrode sensors capable of sensing coating degradation using the AC Impedance technique have been designed and tested with success on aircraft metal/coating systems. These in-situ electrode sensors and their potential applicability for nondestructive, real-time analysis of coating degradation, represent an opportunity to develop a straightforward commercial sensor in a Phase II effort which will ultimately reduce maintenance and down-time of aircraft while increasing flight safety.

If there are any questions or revisions to the report, please do not hesitate to contact me.

Sincerely

Chester M. Dacres, Ph.D., P.E.
President

TABLE OF CONTENTS

SUMMARY:

Electrochemical corrosion testing using AC impedance measurement, ellipsometry, and X-Ray Photoelectron Spectroscopy (XPS) has been performed on aluminum 2024-T3 samples. Electrochemical impedance measurements were used to acquire a precise impedance signature which will be used in a Phase II effort to develop a simple, yet powerful, sensor for the early detection and measurement of corrosion processes on aircraft. The objective of this Phase I project was to show that a distinct signature obtained from a corroding aircraft surface can be used to develop a sensor.

The data show that the painted aircraft aluminum 2024-T3 does degrade with a distinct signature which corresponds to the following plot in Figure 1. There are definite regions on the corrosion spectrum showing water uptake, incubation, and intense corrosion activity. The use of ellipsometry and DC electrochemical techniques have verified the results obtained from the AC Impedance technique. Phase I has proven the feasibility of using the AC Impedance technique to recognize the distinct degradation pattern for aircraft materials.

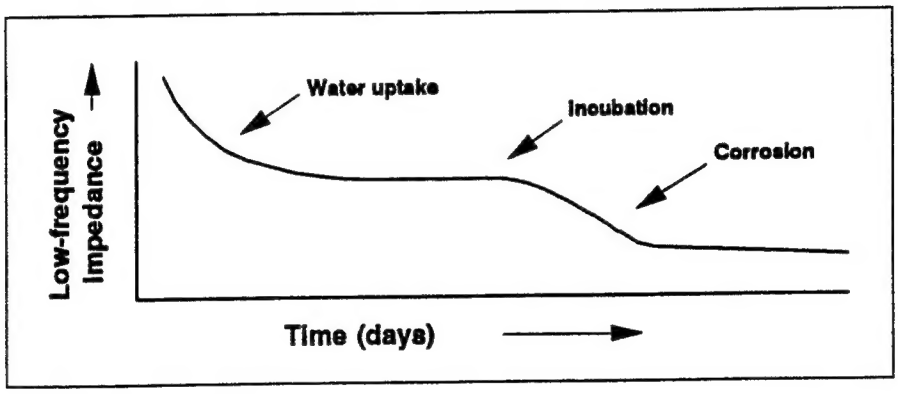

Figure 1. *Corrosion process for painted aircraft aluminum Al 2024-T3.*

Several versions of prototype electrode sensors have been developed in the Phase I effort to obtain this signature utilizing a two-electrode approach. Conventional AC Impedance testing requires the use of three electrodes and an electrolyte making in-situ analyses difficult to perform. Our two-electrode approach eliminates the need for an electrolyte and enables reliable in-situ real-time analyses of aircraft metal/coating systems. Results show that the electrodes are capable of detecting the characteristic corrosion signature. Developing a straightforward sensor based on this pronounced signature using inexpensive electrodes is very feasible.

DACCO SCI, INC. believes the sensors would provide the Air Force with the necessary information to improve maintenance quality, while decreasing its costs and the number of failures due to corrosion.

INTRODUCTION:

Studies by the National Bureau of Standards (NBS) estimate that overall corrosion costs in the United States are 4.2% of the Gross National Product (GNP) or $160 billion in 1986.[1] Overall corrosion costs for the United States Air Force alone are estimated to be greater than one billion dollars each year.[2] Furthermore, it has been estimated that 90% of maintenance problems at Air Force Air Logistics Centers (ALC) are for the remediation of corrosion induced problems.[3] The mitigation of corrosion to extend the operational life of equipment and to increase operator safety is paramount.

Aircraft structures are susceptible to corrosion caused by runway salt, exhaust fumes, oil/gasoline/diesel fuel spills, and cleaning solvents. An increasing percentage of aging Air Force and commercial aircraft maintenance costs are attributable to corrosion. Increased effort will be required to maintain adequate safety standards in the face of the increased structural deterioration of aircraft with operational lifetimes stretched beyond those expected of aircraft at the time they were built. New construction of aircraft will be expected to remain operational for longer operational lifetimes, so early corrosion detection monitors should be built into the aircraft and corrosion-prone structures should be avoided in the design of new aircraft as much as possible.

The Department of Defense (DoD) has addressed several issues involving corrosion, including cathodic protection (sacrificial anode or impressed current) of concrete reinforcements, applications of improved coatings, such as powder coatings, and inspection/maintenance/repair of coatings and structures. Painting remains the most common method of protecting metal structural elements. However, paint is not a permanent solution. It can be damaged to expose bare metal and it is an imperfect barrier to moisture and other corrosion-inducing fluids. Once corrosion begins, the paint can hide the degradation until it becomes severe with blistering and other visible deterioration. The incipient step in corrosion of a painted metal is de-adhesion of the paint/primer as moisture penetrates the polymer and reaches the metal surface.[4] This de-adhesion occurs initially because the metal (oxide) surface prefers to form bonds with water rather than with polymers;[5] it extends and propagates as cathodic corrosion occurs at the interface. At first the de-adhesion is reversible; but as corrosion products form at the interface, the paint blisters and is no longer protective. When exposed to moisture, either by immersion or high humidity, the near-dc impedance of the paint/metal system decreases by one to two orders of magnitude. Identical results can be obtained using ellipsometry, external electrodes, or the grid electrodes in immersion control studies that validated the design and operation of the sensor.

Coating failure involves both the transport of water and a reducible species through the coating and oxidation and reduction reactions at the metal/coating interface. For this reason, electrochemical methods have been the logical choice in the analysis of coating failure. The AC Impedance technique, also known as Electrochemical Impedance Spectroscopy (EIS), is a nondestructive method to evaluate coating failure. Impedance parameters, including coating capacitance, pore resistance, and low frequency impedance can be measured in-situ as a function of time to monitor coating quality. AC impedance techniques use very small excitation amplitudes, generally in the range of 5 to 10 mV peak-to-peak, which provide typical curves called electrochemical impedance spectra. These spectra represent distinct signatures of metal/coating systems.

The aim of the Phase I project is to show that the AC Impedance technique is an accurate and reliable way to detect corrosion on aircraft. Furthermore, the goal of the project is to develop in-situ electrodes capable of monitoring corrosion without the need for both a counter electrode and an electrolyte. Our proposed corrosion monitor sensor will vastly improve an inspector's ability to detect corrosion and paint degradation in its early stages, allowing prompt local remedial action that should reduce the need for expensive wide-area repainting. Such a monitor will also allow a repainting schedule based on the measured potential for material damage and not visible, extensive damage or fixed time intervals. Consequently, the maintenance schedule will be proactive rather than merely responsive to failures.

Ellipsometry, potentiodynamic scans, X-ray Photoelectron Spectroscopy (XPS), and salt spray testing have been used to verify that the AC impedance spectra are representative of the actual corrosion process of aircraft metal/coating systems.

Ellipsometry makes sensitive optical measurements of the surface of samples, and is capable of monitoring the integrity of a coating by noticing any changes in the thickness and refractive index on the surface of the specimen. The ellipsometer also permits simultaneous AC Impedance testing to correlate changes in impedance with changes in the refractive index of a sample. For these reasons, ellipsometry was used to verify the results obtained from the AC Impedance technique.

DC potentiodynamic scans of a sample provide an indication of the corrosive behavior of the specimen in a test solution environment. A potentiodynamic scan involves sending a current through the specimen and measuring the electrochemical reactions at the interface between the metal and the electrolyte. The corrosion rate of the specimen can be calculated by analyzing the oxidizing and reducing reaction rates at the interface. Results obtained from the AC Impedance technique were compared with corrosion rates from the potentiodynamic scan to further verify the accuracy of the results.

X-ray Photoelectron Spectroscopy was used to provide elemental and chemical analysis of the specimens. XPS uses x-rays to excite photoelectrons. The relationship between the measured kinetic energy of the emitted electron and the initial state binding energy identify the element from which the electron was emitted. The energy shifts and the photoelectron lineshape identify the chemical species. This technique provided surface analysis of the corroding specimen to correlate with the AC Impedance data.

Salt spray testing was used to accelerate the corrosion process of the test specimens in order to monitor the entire corrosion process (water uptake, incubation, and active corrosion). Salt spray testing also provided data on the ability of the conductive paint electrodes themselves to withstand harsh environments.

Background discussions of the following techniques utilized in this research project are provided for:

- Electrochemistry
  - *Electrochemical Impedance Spectroscopy (EIS)*
  - *Potentiodynamic Testing*
- Ellipsometry
- Salt Spray (Fog) Testing
- X-Ray Photoelectron Spectroscopy (XPS)
- Scanning Auger Microprobe (SAM)

Electrochemistry - Electrochemical Impedance Spectroscopy

Overview

The electrochemical impedance testing in conjunction with the ellipsometry and the X-ray Photoelectron Spectroscopy provides a method of determining the type of impedance signal to anticipate when painted aircraft aluminum 2024-T3 corrodes. The AC impedance measurements provide a wealth of kinetic and mechanistic information. For this reason, the technique has become very popular for the study of corrosion.

AC impedance techniques use very small excitation amplitudes, generally in the range of 5 to 10 mV peak-to-peak, which provide typical curves called electrochemical impedance spectra. Excitation amplitudes of this magnitude cause only minimal perturbation of the electrochemical test system, thus reducing errors caused by the measurement technique itself. Since AC impedance experiments can provide data on both electrode capacitance and charge-transfer kinetics, the technique offers valuable mechanistic information. In addition, because the method does not involve a potential scan, measurements can be made in low conductivity solutions where DC techniques are subject to serious potential control errors.

Theory

Electrochemical Impedance Spectroscopy (EIS) is based on the fact that the behavior of an electrochemical cell and an electronic circuit is analogous. This allows circuit modelling of a given electrochemical cell. Fundamental AC circuit theory can then be applied to the circuit model and the results can be accurately correlated to reveal physical and chemical properties of the electrochemical cell.

DC theory is defined by Ohm's Law where the frequency is equal to 0 Hz. Ohm's Law states that:

$$E = IR \qquad (1)$$

where E = dc potential (volts)
I = measured current (amps)
R = resistance (ohms)

In AC theory, however the frequency is non-zero. The analogous equation is given by:

$$E = IZ \qquad (2)$$

where E = potential (volts)
I = current (amps)
Z = impedance (ohms)

In an electrochemical cell, the coating, electrolyte, and diffusion, act to slow the flow of electrons and each can be modelled as resistors, capacitors, inductors or a combination of elements. These factors give rise to a particular circuit for a given electrochemical cell. Impedance of circuit elements is defined as:

$$\begin{aligned} &\text{Resistor} && Z = R \\ &\text{Capacitor} && Z = 1/j\,\omega C \\ &\text{Inductor} && Z = j\omega L \end{aligned} \qquad (3)$$

where R = resistance (ohms)
j = imaginary component ($\sqrt{-1}$)
ω = angular frequency (rad/sec) = $2\pi f$
f = frequency (Hz)
C = capacitance (farads)
L = inductance (henries)

Once the system is modelled as a circuit, the characteristics of the circuit can be monitored and evaluated. The equivalent circuit of the coating/metal system can be seen in Figure 2.

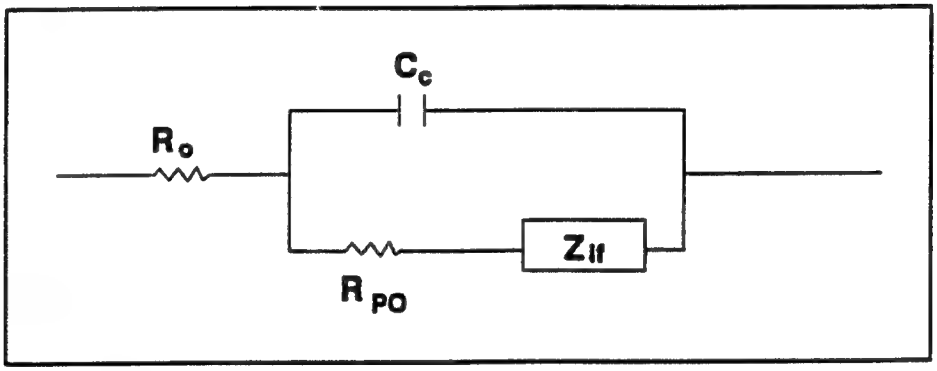

Figure 2. *Equivalent circuit model (ECM) for aircraft metal/coating system.*

The following characteristics are defined as follows:

R_o - ***solution resistance***
This value is the ohmic or uncompensated resistance between the working and reference electrode.

R_{PO} - ***pore resistance and ionic conduction in coating***
The pore resistance is a reflection of the amount of penetration by the electrolyte into the coating.

C_c - ***coating capacitance***
The coating capacitance is used as a measure of the effectiveness or integrity of a coating.

Z_{if} - ***metal interfacial impedance***
This value comprises impedance components associated with electrochemistry at the coating/metal interface, like double layer capacitance, diffusion controlled processes and faradaic reactions.

Graphical Interpretation

Typical results from electrochemical testing of a coated metal substrate can be seen in Figures 3-5. These graphs reveal distinct signatures for each specimen.

Valuable information from electrochemical testing comes from the Bode magnitude plot. The frequency of the sine wave that is sent through the coating/metal system is varied from low to high frequencies (0.01 Hz - 100k Hz). The response of the system to this excitation reveals important characteristics of the modelled circuit. This information is best expressed in the Bode magnitude plot. The Bode magnitude plot (Figure 3) is interpreted as follows:

At low frequencies (< 0.1 Hz) the plot asymptocially approaches a maximum impedance (Z_{if}) where the modelled circuit is resistive. This is because at low frequencies the impedance of a capacitor ($Z = 1/2\pi fC$) approaches infinity and acts as an open circuit, thus eliminating the capacitance almost entirely. At this point the phase angle is zero, and, likewise, the imaginary component of the impedance is zero.

At intermediate frequencies (0.1 Hz - 100k Hz) the impedance due to the coating capacitance becomes more active. The phase angle approaches a maximum of 90 degrees (purely capacitive). The imaginary component of impedance, likewise, reaches a maximum phase angle of 90°.

At the high frequencies (> 100k Hz) the plot asymptocially approaches a minimum impedance. At high frequencies the impedance of a capacitor ($Z = 1/2\pi fC$) approaches zero and acts as a short in the circuit. This reduces the equivalent circuit to the electrolyte resistance, R_o, which explains the bottom plateau.

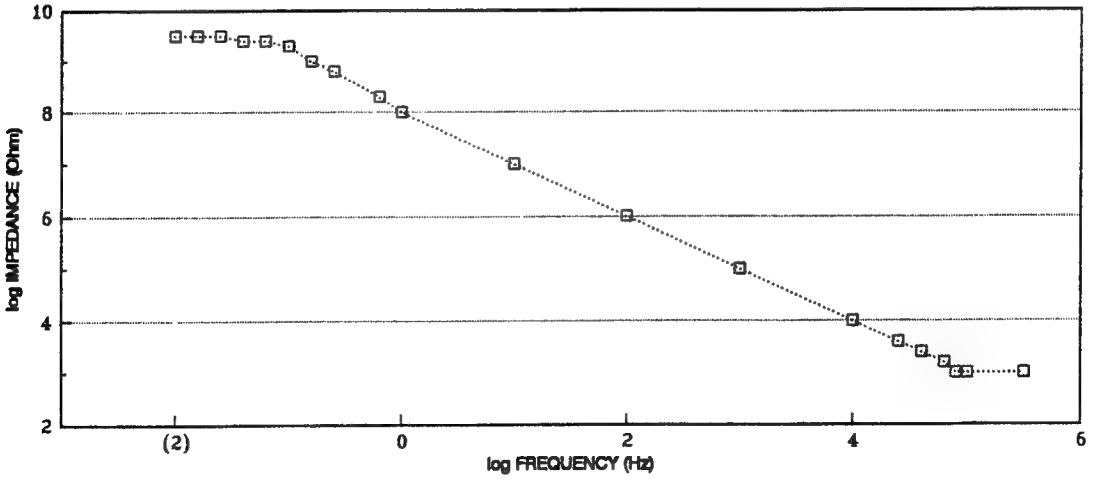

Figure 3. *Typical Bode magnitude plot.*

The Bode Phase Plot (Figure 4) and the Nyquist Plot (Figure 5) can be derived from the Bode Magnitude Plot, displaying the same data but in different graphical form. Both are useful in confirming results found from the Bode Magnitude Plot.

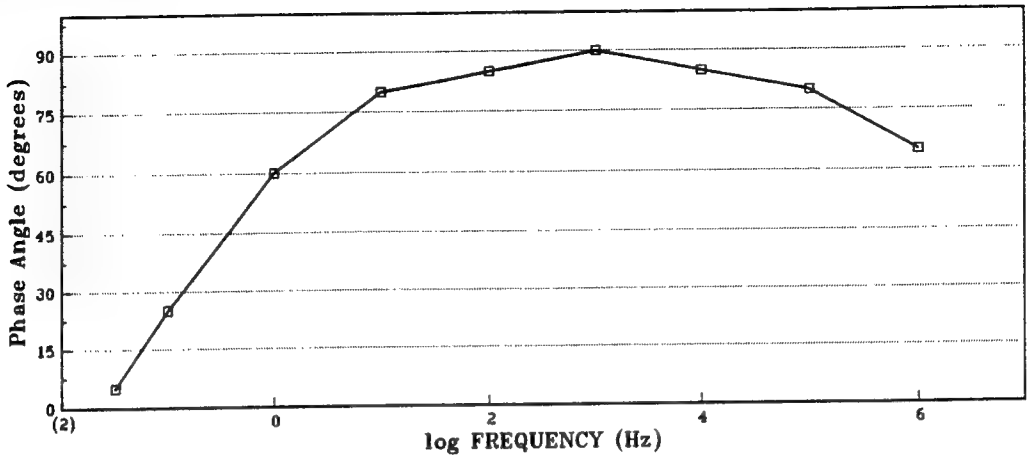

Figure 4. *Bode phase plot for coated aircraft aluminum.*

The Bode plot is a useful alternative to the Nyquist plot by avoiding longer measurement times associated with low frequency determinations.

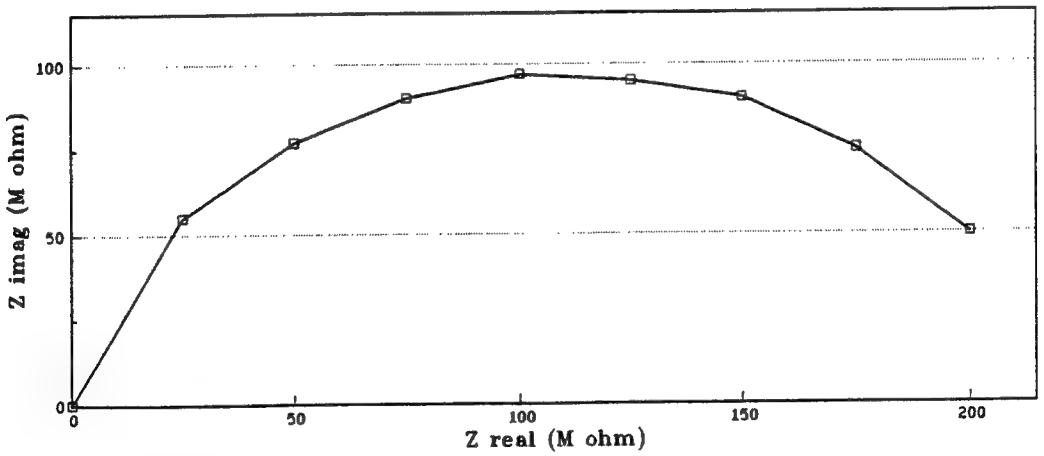

Figure 5. *Typical Nyquist plot of coated aircraft aluminum.*

The primary advantage of the Nyquist plot format is that it is easier to see the effects of the ohmic resistance. The shape of the curve does not change when the ohmic resistance changes. Consequently, it is possible to compare the results of two separate experiments which differ only in the position of the reference electrode.

Coating Capacitance

Coating capacitance, C_c, is a measure of a coating's integrity. The coating/metal interface acts as a capacitor. Thus, as the circuit capacitance increases, the performance of the coating decreases. The determination of a specimen's coating capacitance can be determined graphically or numerically.

Coating capacitance is found at the intermediate frequencies where the slope of the plot (log frequency vs. log impedance) is equal to -1. Numerically C_c is found from the fundamental impedance equation for capacitors where:

$$Z = \frac{1}{jwC} \tag{4}$$

$$\log(Z) = -\log(w) - \log(C) \tag{5}$$

$$\log(Z) = -\log(2\pi f) - \log(C) \tag{6}$$

$$At\ f = .16\ Hz,\ 2\pi f = 1\ and\ \log(1) = 0 \tag{7}$$

$$\log(Z) = -\log(C) \tag{8}$$

$$Z = 1/C \tag{9}$$

$$C = 1/Z \tag{10}$$

C_c is found from the Bode magnitude plot (Figure 6). C_c is calculated as the inverse of the impedance at a frequency of .16 Hz or -.8 Hz on log scale. Extensive testing of samples with a range in corrosion severity will lead to unique values for C_c.

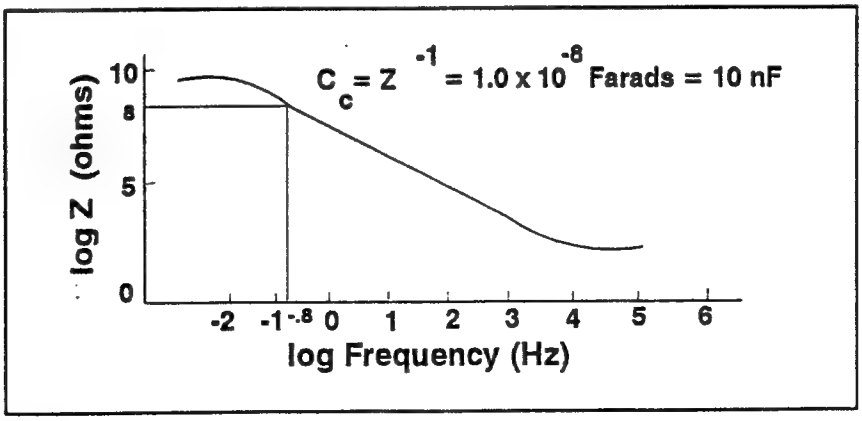

Figure 6. *Determination of coating capacitance from Bode Diagram.*

Water Uptake

Another measure of the severity of corrosion is the amount of water uptake (Figure 7). Ideally, a coated metal would not absorb any water and be completely non-corrosive. However, water is absorbed through pores into the coating which ultimately leads to corrosion. The amount of water uptake is calculated as follows:

$$\%water(volume) = \frac{100\log(C_t/C_o)}{\log(79)} \qquad (11)$$

where

C_t = Coating capacitance at final time
C_o = Coating capacitance at initial time

Like coating capacitance, the severity of corrosion will uniquely depend on the amount of water uptake. Again, samples will exhibit specific signatures which can be easily translated into a coating integrity.

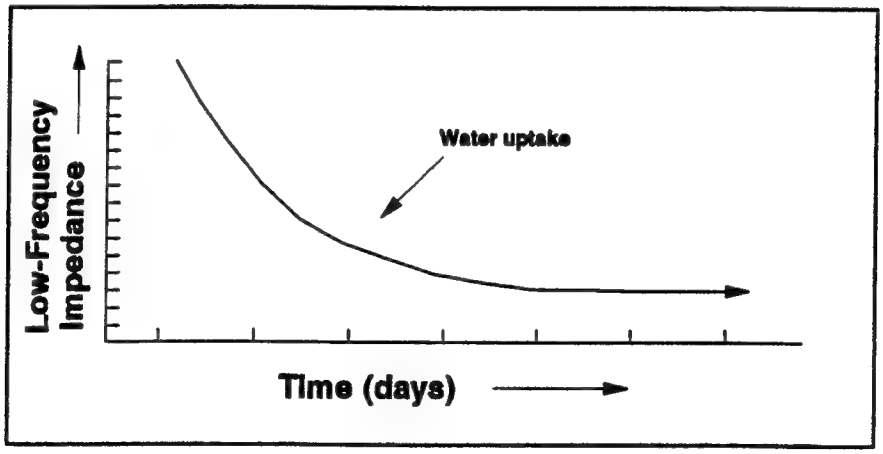

Figure 7. *Anticipated corrosion process for initial water uptake.*

Instrumentation

The Model 398 Electrochemical Impedance System was used to investigate coating integrity of metal systems. This system employs two methods to gather data over the desired frequency range:

(1) the FTT (fast Fourier transform) technique for measurements from 0.0001 Hz to 11 Hz; and

(2) phase-sensitive lock-in detection for measurements from 5 Hz to 100 Khz.

As part of the system, the microcomputer can merge in the data from the FTT and the phase-sensitive lock-in detection in sequence. This enables data acquisition over the entire frequency range. A block diagram of the system is displayed in Figure 8.

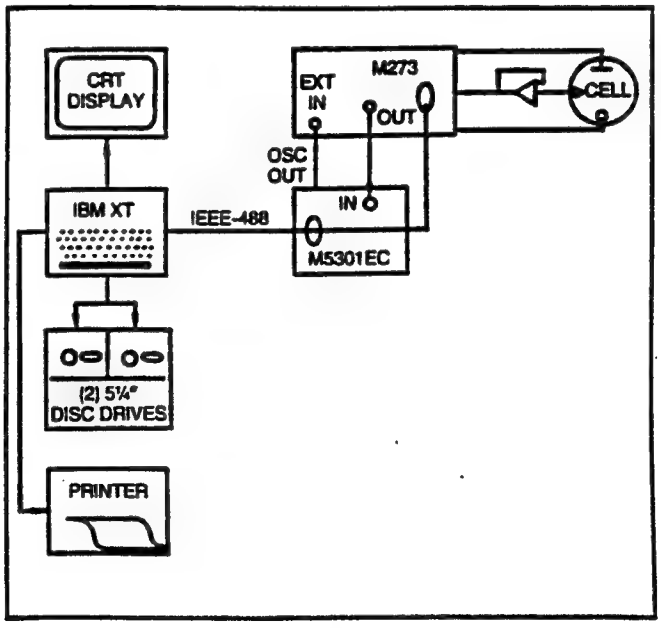

Figure 8. *Block Diagram of the EG&G PAR Model 398 Electrochemical Impedance System capable of obtaining impedance spectrum of painted aircraft aluminum.*

Electrochemical Testing - DC Potentiodynamic Scans

Overview

DC potentiodynamic scans of a sample provide an indication of the corrosion behavior of the specimen in a test solution environment. A potentiodynamic scan involves sending a current through the specimen and measuring the electrochemical reactions at the interface between the metal and the electrolyte. The corrosion rate of the specimen can be calculated by analyzing the oxidizing and reducing reaction rates at the interface. DC corrosion techniques actually induce corrosion in a test sample and provide information on the corrosion rate and the open circuit potential of a given test sample.

The DC corrosion technique will aid in verifying the results obtained from the AC Impedance technique by correlating the severity of corrosion with the corrosion rate itself.

Theory

DC electrochemical corrosion techniques are used to characterize the overall corrosion behavior of a system. A potentiodynamic scan of a specimen provides information on the open circuit potential and the corrosion rate of a sample in a given electrolyte environment.

The potentiodynamic technique (Figure 9) sweeps the potential of a metal specimen slowly over a given potential range. During this sweep, the sample will undergo various electrochemical reactions including oxidation and reduction at the interface of the metal and electrolyte. The rates of these electrochemical reactions are analyzed to yield the information on the corrosion potential, corrosion current, corrosion rate, and mechanistic information.

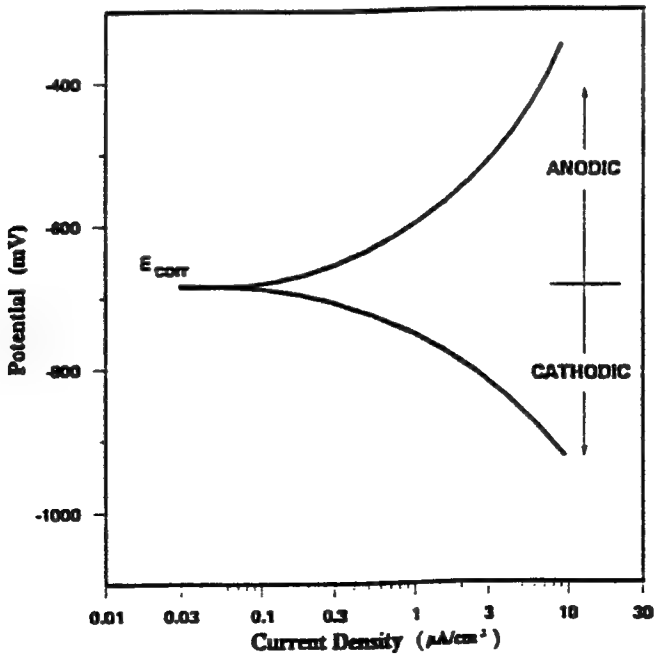

Figure 9. *Potentiodynamic plot of an Al 2024-T3 sample with waterborne epoxy primer.*

At potentials less than E_{corr} the sample is considered to be cathodic. This is the region where reduction occurs at the interface and corrosion is not present. At potentials greater than E_{corr} the sample is considered to be anodic. This region is where the sample undergoes oxidation and begins to corrode. At E_{corr} the anodic current is equal to the cathodic current and oxidation occurs as fast as reduction. This is the point where the sample is in equilibrium.

The data from this plot can then be analyzed to determine the calculated corrosion potential (E_{corr}), corrosion current (I_{corr}), and the corrosion rate (C.R.). First, a nonlinear least-squares fit of the data is used to minimize the difference in the observed and calculated results according to the following equation:

$$\chi^2 = \frac{\sum [(I_{obs,i} - I_{calc,i}) / s_i]^2}{N - 4} \qquad (12)$$

where N = total number of points
s_i = standard deviation of the i^{th} current value
$I_{obs,i}$ = observed current at the i^{th} data point
$I_{calc,i}$ = current calculated from the Stearn-Geary equation and the corrosion parameters

The least square fit continues until there is a deviation of only 0.1% between χ^2 iterations.

The corrosion rate of the sample is quickly determined from the above results according to the following equation:

$$C.R. = C\ (EW / d)\ (I_{corr} / A) \qquad (13)$$

where EW = equivalent weight of the sample
A = sample area
d = density of sample
C = conversion constant

Instrumentation

The Model 352 SoftCorr II Corrosion Measurement and Analysis Software was used to perform potentiodynamic scans and analyze the data. The EG&G PAR Model 273 potentiostat was used to apply the potential. The potentiostat was then electrically connected to the EG&G PAR Model K47 electrochemical corrosion cell used for the testing of the samples. The EG&G PAR Model K47 corrosion cell holds two counter electrodes and a reference electrode. The sample is suspended into the solution in the center of the cell by the specimen holder and is electrically connected as the working electrode. A Potassium Chloride (KCl) electrode was used as the reference electrode.

The corrosion cell is displayed in Figure 10.

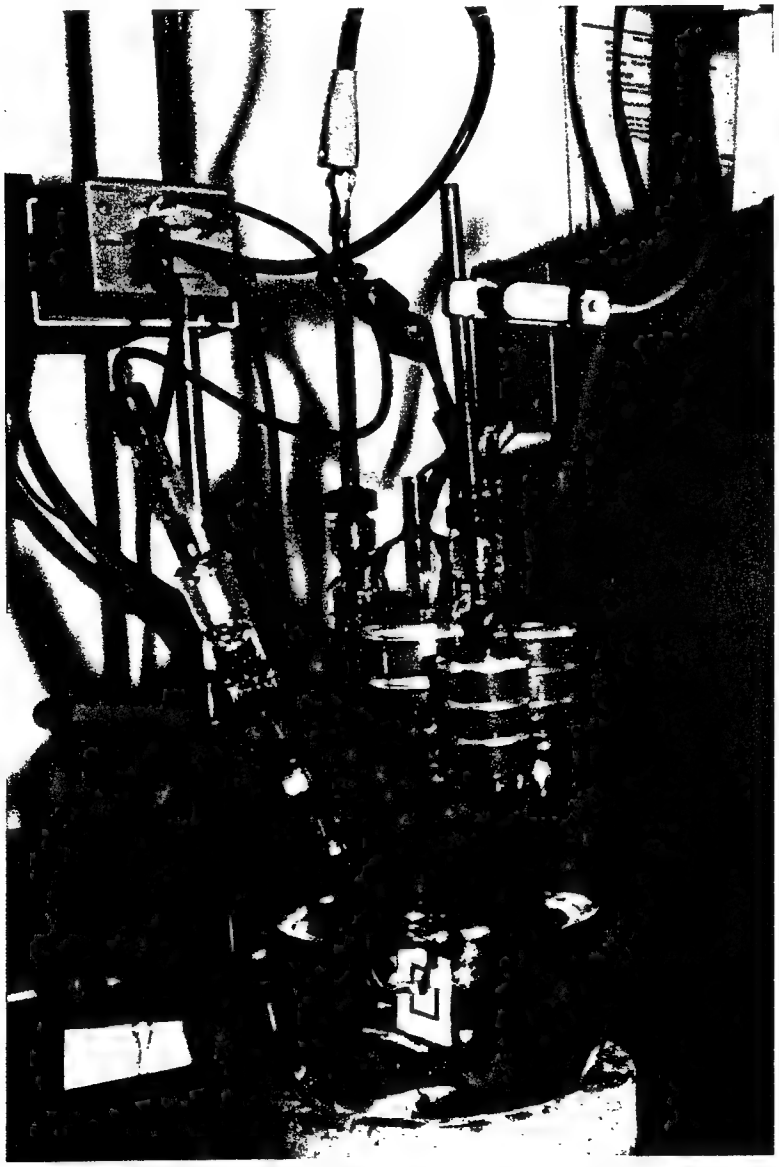

Figure 10. *EG&G PAR Model K47 three-electrode electrochemical corrosion cell.*

Ellipsometry

Overview

Ellipsometry is the measurement of the effect of reflection on the state of polarization of polarized light. Ellipsometry is especially suited for the observation of film formation, integrity, and degradation of metals. The techniques and principles of ellipsometry have been used since the early 1900's. With recent advances in electrochemical testing, the use of ellipsometry has become an increasingly popular tool in the study of corrosion. Furthermore, ellipsometry can be performed simultaneously with electrochemical techniques, such as Electrochemical Impedance Spectroscopy, to provide another technique for analyzing corrosion.

Ellipsometry reflects light of a known polarization from a substrate. The presence of a film or coating will cause the light to change polarization. This change in polarization is then measured and mathematically correlated with optical constants and film thickness. The use of ellipsometry does not accelerate or alter the integrity or formation of coatings. Therefore, it is an accurate method for verifying electrochemical results.

Theory

The state of polarization of light is determined by the phase and amplitude of the incident and reflected light. The characteristics of these waveforms are illustrated in Figure 11. In this illustration the reflected light is polarized. This is characterized by the p and s components being in phase. Any difference in the phase, results in the light being elliptically polarized. Thus, reflected light results in an amplitude and a phase change. The change in phase is defined as Δ . The change in the ratios of the amplitude is defined as the tangent of the incident angle ψ, namely:

$$\Delta = (\beta_p - \beta_s)_{reflected} - (\beta_p - \beta_s)_{incident}$$

$$\tan\psi = \frac{(E_p/E_s)_{reflected}}{(E_p/E_s)_{incident}} \qquad (14)$$

Ellipsometry is used to measure Δ and ψ.

The fundamental equation of ellipsometry was derived by Winterbottom who established the relationship between Δ, ψ, and the properties of the reflected light in terms of the Fresnel reflection coefficients (r) for the two component waves and the optical thickness of the film. The equation is given as:

$$(\tan\psi)\, e^{i\Delta} = \frac{r_{1p} + r_{2p} e^{-2i\delta}}{1 + r_{1p} r_{2p} e^{-2i\delta}} * \frac{1 + r_{1s} r_{2s} e^{-2i\delta}}{r_{1s} + r_{2s} e^{-2i\delta}} \qquad (15)$$

The quantity δ is the change in phase of the reflected light with a wavelength λ caused by traversing the coating of thickness d and index of refraction n_1.

$$\delta = (360/\lambda)\, d(n_1^2 - n_o^2 \sin^2\phi)^{.5} \quad degrees \qquad (16)$$

where ϕ = angle of incidence
n_o = index of refraction of ambient medium

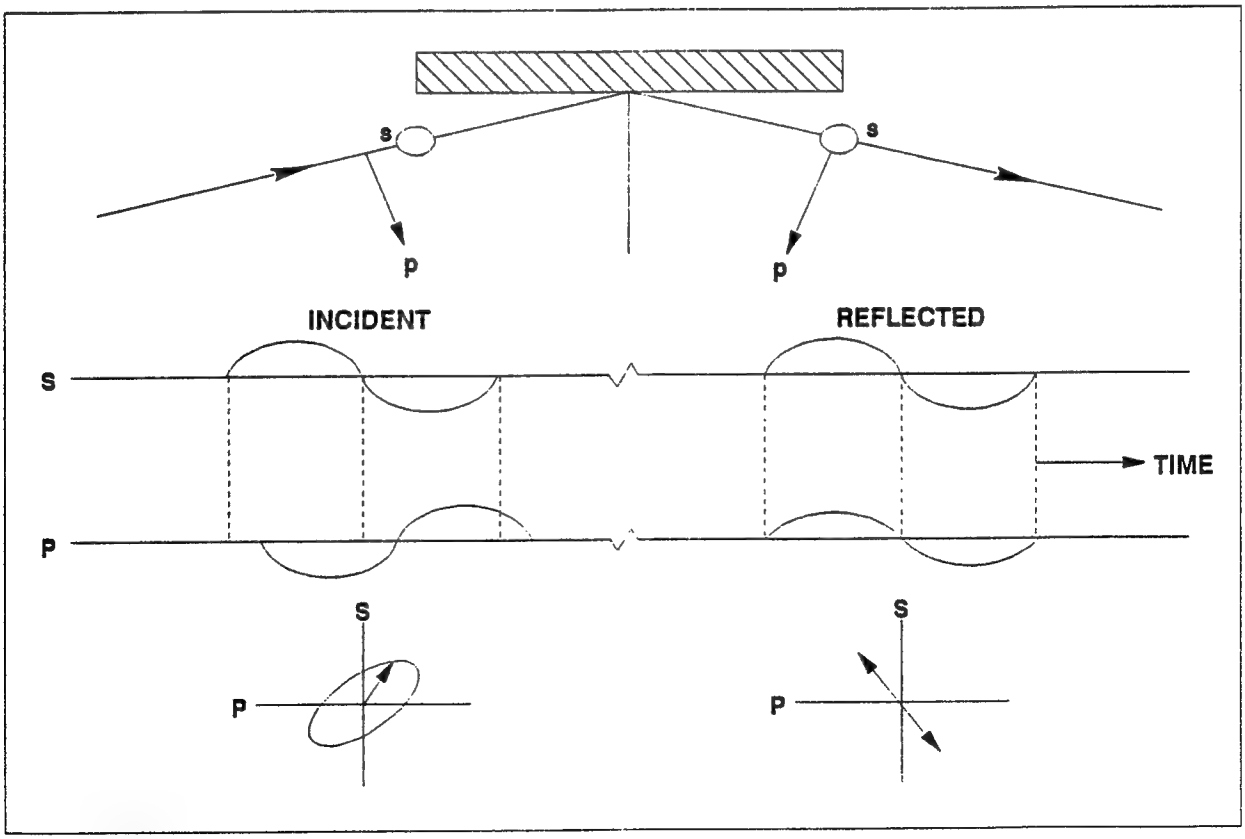

Figure 11. *Resolution of incident and reflected beams into p and s components.*

The general formula for the Fresnel coefficients is given as:

$$r_p = \frac{n_a \cos\phi_b - n_b \cos\phi_a}{n_a \cos\phi_b + n_b \cos\phi_a} \qquad r_s = \frac{n_a \cos\phi_a \, n_b \cos\phi_b}{n_a \cos\phi_a + n_b \cos\phi_b} \quad (17)$$

where n_a, n_b = indices of refraction of the media
ϕ_a = angle of incidence
ϕ_b = angle of refraction

Substitution of equations 16 and 17 into 15 yields equations for Δ and ψ. Solution of these equations will yield properties of the film. All other variables including the wavelength, the index of refraction for substrate and film, and the angle of incidence are either fixed constants or are independently determined.

Due to the complexity of the above equations, computer software has been developed to electronically calculate results.

Instrumentation

Ellipsometry research was conducted using the Gaertner Scientific Model L119X Ellipsometer. A 4mW Helium-Neon (HeNe) laser with a wavelength of 6238 Å was used as the light source. The ellipsometer consists of a quarter wave plate with a removable compensator and a computer controlled analyzer/ photocell detector unit. This unit automatically determines the null point of the incident laser light and eliminates the need for manual adjustment. See Figure 12 for the layout of the ellipsometer.

The measurement time of the film thickness and refractive index takes under one second to complete. The ellipsometer computer program allows a dual measurement (with and without the compensator) for more accurate results with a measurement time of about three seconds.

An optical electrochemical cell can be used in order to monitor both the electrochemistry and ellipsometry of test samples simultaneously (Figure 13). The apparatus consists of a specially crafted optical cell which allows the laser light source to enter the electrochemical cell, pass through the electrolyte, reflect from the test specimen, and continue out of the cell to the photocell. This permits AC impedance techniques to be applied while optically monitoring any changes in the surface of the coating. It is for this reason the optical electrochemical cell is important in verifying results found from electrochemical techniques. The amount of water uptake and any de-adhesion in the coating can be verified using ellipsometry.

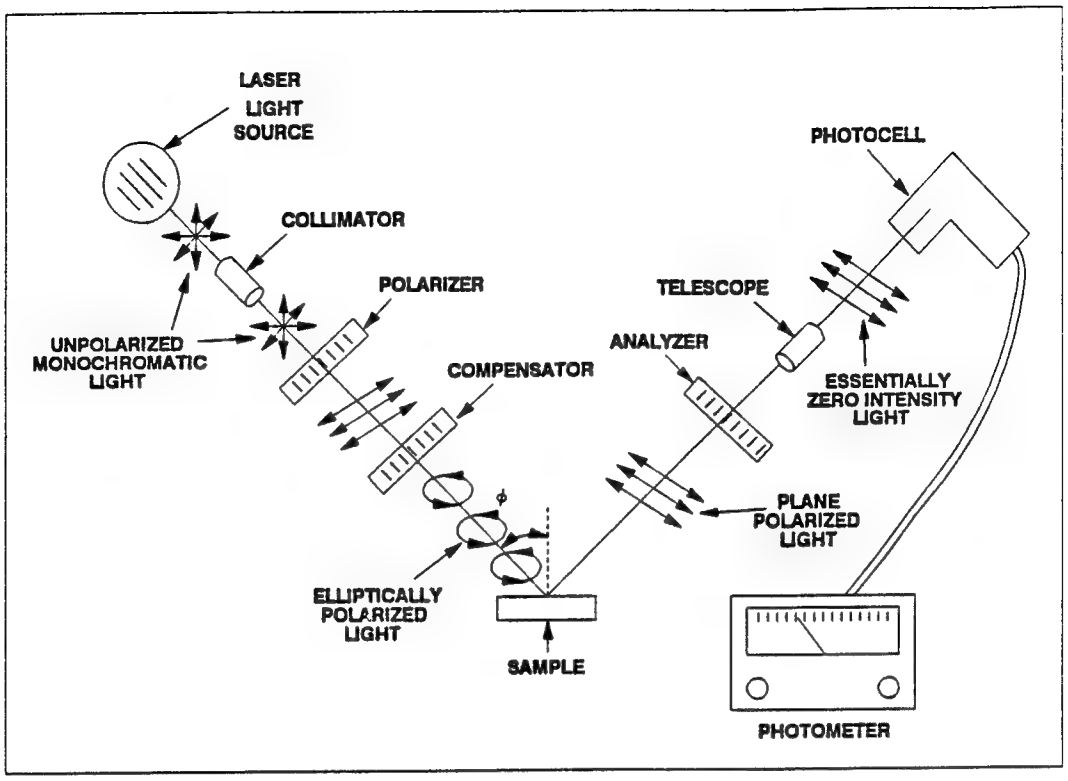

Figure 12. *Components of an ellipsometer.*

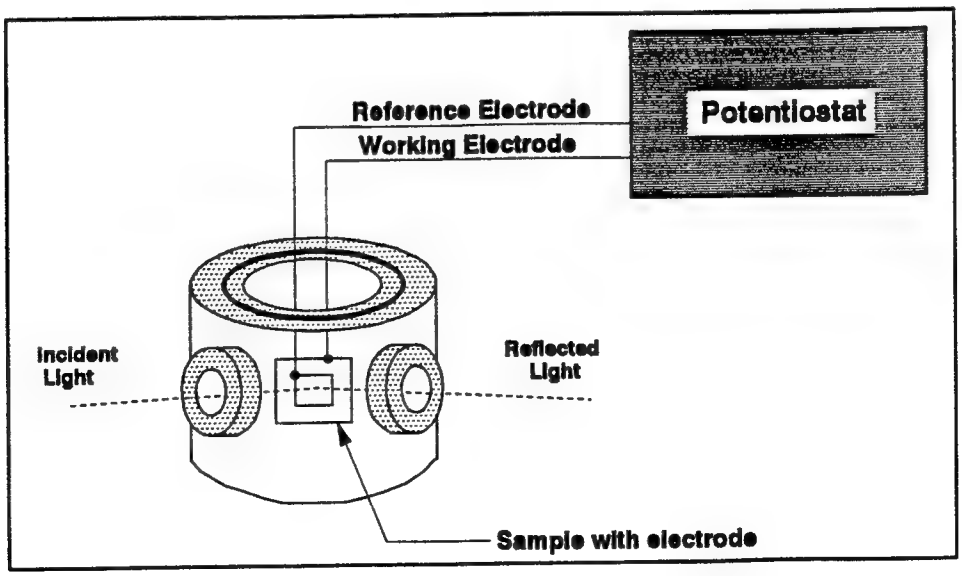

Figure 13. *Optical electrochemical corrosion cell.*

Salt Spray (Fog) Testing

Overview

Salt spray testing is typically used to measure the corrodibility of nonmetallic and metallic coatings. The testing is accomplished by accelerated corrosion of a sample as opposed to time-consuming field testing. A given lot of samples is exposed to an elevated temperature and salt spray for a set time. This procedure simulates the effect of a marine environment.

There is concern that salt fog testing does not necessarily represent actual corrosion processes that would occur in a normal environment. While it is true that results obtained from salt spray testing are difficult to reproduce and do not represent actual corrosion scenarios, it is the net result which is desired, that the samples experience accelerated corrosion and physically and chemically become altered. These samples with accelerated corrosion can then be electrochemically tested using the AC Impedance technique on the painted electrodes to detect the amount and severity of corrosion of the coating. Furthermore, the ability of the painted electrode itself to withstand harsh environments will be determined.

Instrumentation

The Singleton Corporation SCCH Corrosion Test Cabinet Model 20 salt spray cabinet (Figure 14) is used to test the inorganic coating on the samples. The apparatus is approximately six (6) feet in length, four (4) feet in width, and four (4) feet in height. The exposure chamber is capable of holding 20 electrode samples for a single test. This model uses a 5% NaCl solution at a operating temperature of 99°F in the exposure chamber.

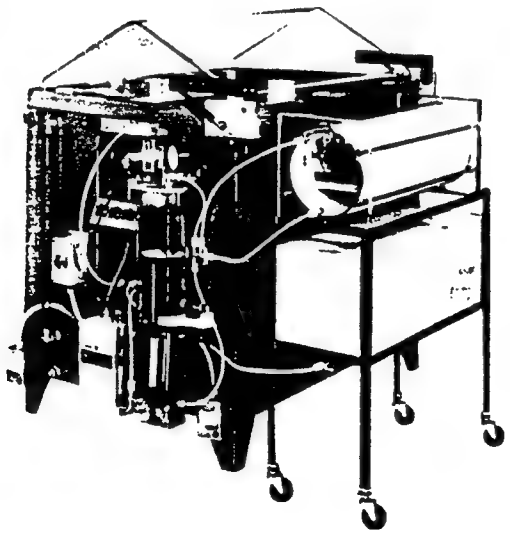

Figure 14. *Salt spray cabinet.*

X-ray Photoelectron Spectroscopy (XPS)

Overview

X-ray Photoelectron Spectroscopy, which is also known as Electron Spectroscopy for Chemical Analysis (ESCA), provides elemental and chemical analysis of specimens. The technique uses low energy x-rays to excite photoelectrons and to create core electronic level holes in materials to depths of the order of 1-3 μm. The modes for de-excitation of the electronic core holes are either the emission of lower energy soft x-rays or Auger electrons. Both the emitted photoelectrons and the Auger electrons have energies commonly below 1500 eV and have large cross-sections for inelastic loss processes. The elastically emitted electrons then are almost entirely emitted from depths of less than 5 nm (or 50 Å) into the material. Half of them might commonly be emitted from depths of 1 to 2 nm, depending on the energy of the emitted electron and the angle between the surface normal and the electron energy analyzer/detector. A spectrum consists of the number of detected electrons (both primary photoelectrons and Auger electrons and inelastically scattered or secondary electrons from those processes) vs. their energy.

Theory

Photoelectrons are characterized in terms of the binding energy of the electronic level from which they were excited. The relationship between the measured kinetic energy of the emitted electron and the initial state binding energy is $E_B = E_X - E_K - \Phi$, where E_B is the binding energy, E_X is the x-ray energy, E_K is the emitted electron kinetic energy, and Φ is the effective work function of the electron energy analyzer (a value of 4 or 5 eV commonly). Photoelectron binding energies identify the element from which the electron was emitted. The local chemical environment around the atom causes small energy perturbations which are characteristic of the chemical bonding and local electronic charge densities. Frequently, the energy shifts and the photoelectron lineshape identify the chemical species.

An Auger electron transition requires that one electron fall from a higher energy state into the x-ray created electron hole while another electron in an occupied level is excited and carries away the energy difference between the other two levels minus the energy needed to overcome its own binding energy. The Auger electrons for a given electronic transition are characterized by the electron kinetic energy for a given element. The kinetic energy of the emitted Auger electron is then given by the relationship, $E_{K3} = E_{B1} - E_{B2} - E_{B3} - \Phi$. The E_B's are the binding energy of (1) the initial electronic level core hole, (2) the newly created hole whose electron has de-excited the initial core hole, and (3) the binding energy of the electronic level whose electron is emitted as the Auger electron. The energy of the emitted electron is seen not to depend on the energy of the x-ray which started the whole process by creating a core hole. Again, lineshapes and energy perturbations for an Auger electron can carry information about the chemical species involved. Commonly the chemical information is more masked by the fact that an Auger transition is the result of an interaction of electrons from three electronic energy levels. Consequently, it is usually broader than a photoelectronic emission process and multiple co-existing chemical species can more often hide out in the overlapping spectra.

The quantitative results are deduced from the area measured under XPS peaks for each element present. When more than one peak for an element is present and unobstructed by overlapping peaks of other elements, a consistency check can be made on the quantitative results by basing calculations on each peak. The calculation is based on sensitivity factors which account for the photoionization cross-section for the given element and its electronic level, corrected for the inelastic mean free path for the photoelectron or Auger electron, and the transmission function of the electron energy analyzer. Usually the assumption of an uniform distribution with respect to depth is made for each element throughout the XPS analyzed volume for the purposes of producing a quantitative result. This is frequently not the case. There are often strong concentration gradients at a surface or at an interface even within the depth probed by XPS. There are means to produce analyses based on models of the inhomogeneous depth distribution with information produced from angle-resolved XPS which is discussed below. These analyses are usually beyond the means of short-term projects, however. Where the characteristics of roughly similar samples require differentiation, the assumption of uniform depth most frequently will not obliterate important trends.

When information about the distribution of species as a function of depth is desired, two techniques are readily available. The first is variable angle resolved XPS. In this technique, the electron take-off angle with respect to the surface is varied with the result that the signal strength is proportional to $d/\sin\theta$, where d is the depth of the emitting atom beneath the surface and θ is the angle between the plane of the sample surface and the direction of the emitted electron. When the species concentration dependence with depth at depths of 5 nm or more is desired, it is necessary to use Ar ion sputtering at energies commonly from 1 to 5 KeV to erode away the surface layers. XPS data acquisition is then possible at various depths beneath the initial surface. Usually this technique is only used to depths less than 1 μm. This limitation is due to the apparent broadening of interfaces after heavy ion sputtering, to the contamination of the XPS system by excessive deposition of sample materials sputtered onto the system's surfaces, and by the length of time required to sputter to great depths. The first of these limitations can be greatly minimized by rotating the specimen while sputtering it.

Instrumentation

The XPS system used in this work was the Surface Science Instruments SSX-100 system with a toroidal crystal monochromatized Al x-ray source. The x-ray source produces spot sizes of 150, 300, 600, and 1000 μm. The angle between the monochromatized Al x-ray source and the analyzer is 90° and the x-ray energy is 1486.7 eV. The electron energy analyzer is a 180° spherical capacitor energy analyzer with a position-sensitive detector with 128 sensing elements. The analyzer allows the selection of 25, 50, 100, and 150 Ev pass energies. The system's energy resolution increases as the x-ray spot size is decreased and as the analyzer pass energy is decreased. In each case, the instrument's counting rates also decrease as the energy resolving power is increased.

The survey spectra to identify the elements present on a surface are usually performed at a pass energy of 150 eV and with an x-ray spot size of 600 μm. The step size for the usual 0-1100 eV binding energy range survey is 1.07 eV. Most elements are detectable at concentrations of 0.1 at.% in a survey scan with 1 hour of data acquisition time.

This system provides very high resolution spectra. We have obtained spectra in our laboratory with the measured full width at half maximum (FWHM) on the Ag $3d_{5/2}$ photoelectron line of 0.54 eV. The high resolution spectra are usually made in the scanned mode with a pass energy of 50 eV and an x-ray spot size of 600 μm. In the high resolution case, the step size between data points is usually 0.16 eV.

A small-area focused Ar ion gun provides a calibrated sample erosion rate with rastered sputtering over areas ranging from about 1 mm square to about 6 mm square. The ion gun is differentially pumped to insure that the analysis chamber has a minimum of active vapors present during sputtering. A low energy electron gun is available to neutralize charging potentials which can develop on insulating specimens or in insulating surface films as the result of x-ray induced electron emission. The sample is mounted on a rotatable sample holder of 1" outer diameter. Samples should generally be less than 0.75" in diameter and less than 0.12" high, though samples as high as 0.37" high can be handled if the sample has one other dimension less than about 0.37". Samples longer than 1" can be handled if they are sufficiently narrow (with some difficulty). Samples with two dimensions very slightly larger than 1" can sometimes be "glued" in place on a sample holder using a colloidal graphite suspension. However, this requires additional drying time and sample pumping time in the sample introduction chamber. Two specialized sample staging points on a 5 staging point sample carousel are available: one is electrically insulated from the carousel and the other can heat samples to 500C.

A base analysis chamber pressure of less than 3×10^{-9} Torr insures that superficially adsorbed vapors on surfaces are removed and reduces the possibility of contaminant vapor adsorption on surfaces during analysis. The analysis chamber is principally pumped by a 240 l/s ion pump with an auxiliary titanium sublimation getter pump which can handle a relatively large vapor output. A sample introduction chamber which is separately pumped by a 50 l/s turbomolecular pump prevents exposure of the analysis chamber to heavy gas loads upon the introduction of new samples. After the pressure in the sample introduction chamber is brought below 1×10^{-6} Torr, the sample is passed into a sample preparation chamber which is pumped by a 120 l/s ion pump. The base pressure in this chamber is less than 3×10^{-9} Torr and it is not allowed to rise above 1×10^{-6} Torr during the introduction of a sample into this chamber. When samples are next introduced into the analysis chamber, the pressure is not allowed to rise above 4×10^{-7} Torr. This sample introduction process is very effective in eliminating contamination of the vacuum system and the cross-contamination of samples. The sample analyses are routinely performed at pressures below 2×10^{-7} Torr for applied technology specimens and below 5×10^{-8} Torr for research quality specimens.

Sputter depth profiles can be performed while rotating the specimen to provide maximal depth resolution. The use of specimen rotation while ion sputtering a specimen greatly reduces ion bombardment induced surface roughening via such phenomena as cone formation induced by formations of slow-sputtering atoms on top of fast-sputtering atoms.

The analysis chamber is equipped with a 0 - 300 amu residual gas analyzer (RGA) of the quadrupole type with both an electron multiplier detector and a Faraday cup. The RGA is controlled from the Windows 3.1 GUI of a PC. This RGA is used to determine what species are desorbing from specimens due to the high vapor pressure of the species, the heating of the specimen, or the ion bombardment of the specimen. The RGA analysis of desorbing species as a function of time complements the XPS analysis of the specimen surface as a function of time while pumping on the specimen, heating it, or ion bombarding it. The RGA serves to check for the possibility of contamination of specimens either from other specimens or due to problems of the vacuum system itself. It is also very useful for leak checking the system.

The XPS setup is displayed in Figure 15.

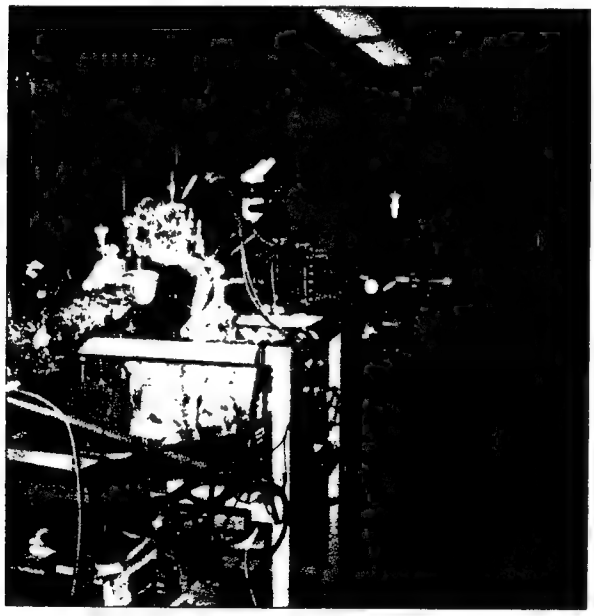

Figure 15. *XPS setup.*

Scanning Auger Microprobe (SAM)

Overview

SAM is the result of a merger of the Scanning Electron Microscopy (SEM) technique and the surface analysis technique known as Auger Electron Spectroscopy (AES). The scanning Auger microprobe technique rasters an electron beam, commonly having an energy of 2-10 KeV, over the analysis area of a sample. When all the emitted and backscattered electrons are detected with little or no regard for their energy, the detected electron intensity at a given primary electron beam position on the sample is displayed. This produces the traditional SEM photomicrograph image of a specimen. While the beam is rastered or while it is held at a stationary point, one can selectively determine the number of electrons of a given emission energy. Most of these electrons are secondary electrons emitted from the sample as the result of high energy electron absorption processes and collisions at depths as deep as 1 μm below the sample surface. Superimposed on this generally slowly varying background of electrons are the Auger electrons, which are emitted as the result of the de-excitation of core holes created by the incident electron beam. The Auger electron emission process competes with the emission of characteristic x-rays to de-excite the core electron holes and is generally the more prevalent process for the low Z elements. As a result, SAM has much greater sensitivity for low Z elements than even windowless EDX.

Theory

An Auger electron transition requires that one electron fall from a higher energy state into the electron hole caused by the electron beam while another electron in an occupied level is excited and carries away the energy difference between the other two levels minus the energy needed to overcome its own binding energy. The Auger electrons for a given electronic transition are characterized by the electron kinetic energy for a given element. The kinetic energy of the emitted Auger electron is then given by the relationship, $E_{K3} = E_{B1} - E_{B2} - E_{B3} - \Phi$. The E_B's are the binding energy of (1) the initial electronic level core hole, (2) the newly created hole whose electron has de-excited the initial core hole, and (3) the binding energy of the electronic level whose electron is emitted as the Auger electron. The energy of the emitted electron is seen not to depend on the energy of the primary electrons which started the whole process by creating a core hole. Monitoring the energy of the emitted electron spectrum from 0 to 2400 eV, allows the identification of all elements except H and He on the basis of their characteristic Auger electron emission lines. Since the inelastic mean free electron path is short for these low energy electrons, the Auger electrons emitted from depths greater than about 50Å appear in the broad background spectrum since they will usually have suffered energy loss in collisions. Those emitted from the surface at the characteristic transition energies, are generally found on a high background. To enhance their detection, one commonly uses lock-in amplifier techniques to amplify the signal of only those electrons having the frequency superimposed on the internal voltages of the energy analyzer. The spectrum this approach yields is an approximation to the derivative of the number of electrons emitted at each energy, and so enhances the signal at the local rapid change in the number of electrons at the characteristic Auger electron transition energies. Pulse counting techniques are also used, sometimes in conjunction with beam brightness modulation of the primary incident electron beam, to measure the Auger

signal, particularly at high spatial resolution when narrow beam diameters limit the beam current sufficiently.

Instrumentation

The SAM system is a JEOL Auger Microprobe JAMP-10S, having a SEM image capability of 25nm and an Auger spectroscopy resolution of 50nm, in principle. Vibrations in the facility, limit the instrument to a resolution of about 50nm. The instrument is equipped with a highly precise eucentric goniometer sample stage, with x, y, and z translation, 360° rotation while normal to the electron beam axis, and 0 - 60° rotation with respect to the beam axis and the 90 - 30° with respect to the energy analyzer axis. The electron beam is generated by a high-brightness LaB_6 electron gun providing a wide range of beam currents from 10^{-5} to 10^{-11} A and an incident beam energy range of 0.1 to 10KeV. The electron optical system consists of a gun bias change mechanism, a double-gap polepiece condenser lens to maintain focus over a wide range of beam currents and voltages, and a low-aberration objective lens. The low voltage range optimization of the electron beam column in this instrument gives it a far greater sensitivity and resolution for shallow features at the surface than that of most SEMs, since most SEMs have a lower limit beam voltage of 5 to 15KeV so that most of their signal comes from hundreds of nm below the surface. A half-cylindrical mirror analyzer determines the electron energy of counted electrons. The system is equipped with both the analyzer voltage modulation and the pulse-counting beam-brightness-modulation detection schemes.

Sample sizes usually need to be less than 26mm in diameter and less than 7mm high. Special sample mounting techniques will allow some sample shapes with one or two larger dimensions to be analyzed. Samples are introduced through a sample introduction chamber equipped with a 170l/s turbomolecular pump for fast pump-down times. The analysis chamber is pumped by a 200l/s ion pump and a 1600l/s titanium sublimation pump. The ultimate analysis chamber base pressure is $<10^{-7}$ Pa or $<10^{-9}$ Torr. In practice, the pressure is usually $<5x10^{-9}$ Torr. The electron optical column is pumped by a separate 32l/s ion pump. The system is also equipped with a differentially pumped ion gun to enable depth profiles to depths as great as 2μm, without straining the analyzer chamber ion pump or introducing backstreaming pump contamination.

The SAM technique yields semi-quantitative elemental analyses with a sensitivity of about 0.1 atomic % for most elements, baring the overlap of the peak Auger energies of two or more elements. The quantitation is either made by measuring the peak-to-peak heights of derivative spectra and dividing these heights with the relative sensitivity factor for each element or by measuring the area under each peak of a pulse-counted spectrum and dividing by a different set of sensitivity factors. The later technique is more accurate, but usually the spectra take longer to acquire. In addition to elemental identification and quantitation, the lineshapes and energy perturbations for an Auger electron can carry information about the chemical species involved. Commonly the chemical information is harder than that of XPS to extract since an Auger transition is the result of an interaction of electrons from three electronic energy levels. Consequently, the Auger transition peaks are usually broader than photoelectronic emission peaks, so multiple co-existing chemical species are harder to resolve in the overlapping spectra which often result. Still, it is usually easy to tell the difference between Si and SiO_2 and

between Al and Al_2O_3, for instance. Finally, because the SAM technique examines very small areas of the sample surface depth profiles to determine the distribution of elements as a function of depth from the top surface are more readily and quickly accomplished, since the ion beam can be focused to a smaller, more intense size. The ion etch rates established can be 10 - 100 greater than those used in conjunction with XPS sputter depth profiles. When a high degree of depth resolution is desired, the sputter area must be increased to decrease the change in depth in the time it takes to acquire the AES spectrum.

The great advantage of SAM over XPS is its much greater lateral spatial resolution. It can also perform depth profiles at a faster rate. However, it suffers by being less accurate quantitatively. It also has a lower sensitivity to most, but not all, elements. XPS is usually less sensitive to low Z elements and AES to the higher Z elements, but other factors can be crucial for real-world samples, such as peak overlaps, background levels, and differing peak energies. Frequently, the two techniques are beneficially applied to the same samples. XPS can rapidly provide the average surface composition, while SAM can show the true heterogeneity of the sample. SAM tends to do more sample damage to sensitive materials, such as photosensitive materials, high ionic conductivity samples, or insulating materials which are locally heated by the electron beam. Also, SAM is more subject to problems caused by surface potentials developing on insulating samples due to the incoming electron beam or the loss of emitted electrons from the sample. This sample charging decreases the SEM and SAM spatial resolution and can prevent the acquisition of AES spectra either wholly or in part of the energy range.

The SAM setup is displayed in Figure 16.

Figure 16. *SAM setup.*

PLAN OF ACTION AND MILESTONES (POAM):

The following proposed plan of action and milestones (Table 1) had been arranged and was adhered to as closely as possible.

Table 1. *Plan of Action and Milestones (POAM).*

TASKS	TIME - MONTHS					
	Jul	Aug	Sept	Oct	Nov	Dec
1) Selection of Candidate Materials						
Al 2024-T3*						
Al 7075-T6						
Anodizations - SAA, CAA						
Mil-P-23377 Epoxy Polyamide Primer*						
Mil-C-85582 Waterborne Epoxy Primer*						
Mil-C-83286 Urethane Topcoat*						
2) Fabrication of Experiment Prototypes						
Control - Remote electrode						
Prototype 1. - Thin gold conductive epoxy applied to the paint topcoat outer surface.						
Prototype 2. - Thin carbon conductive paint applied to the paint topcoat outer surface.						
Prototype 3. - Thin silver conductive paint applied to the paint topcoat outer surface.†						
Prototype 4. - Thin nickel conductive paint applied to the paint topcoat outer surface.†						

* Selected
† Added to scope of work

Table 1 (continued). *Plan of Action and Milestones (POAM).*

TASK	TIME - MONTHS					
	JUL	AUG	SEPT	OCT	NOV	DEC
3) Experimental Preparations						
Salt Fog						
AC Impedance						
Ellipsometry						
XPS						
Samples with Sputtered Grid or Remote Electrode						
No Defect						
Defect						
Samples with Gold, Silver, Carbon, and Nickel Electrodes						
No Defect						
Defect						
4) Experimental Measurements						
AC Impedance - 45 Samples						
Ellipsometry - 20 Samples						
XPS - 10 Samples						
Salt Fog - 20 samples						
5) Data Analysis						
6) Reporting						

SCOPE:

1. To prepare coated aluminum 2024-T3 samples with gold, silver, nickel, and carbon painted electrodes applied to the coating. The substrate and the electrode are fitted with wire electrical hookups.

2. To perform AC impedance measurements using Electrochemical Impedance Spectroscopy (EIS) on Al 2024-T3 samples according to the test matrix in Table 2.

Table 2. *Test matrix for electrochemical impedance spectroscopy in conjunction with other testing.*

		Waterborne Epoxy		Epoxy Polyamide	
Electrode Type	**Samples**	**Ellipsometry**	**Salt Fog/ XPS**	**Ellipsometry**	**Salt Fog/ XPS**
Remote Electrode	**Defect**	4	2	2	2
	No Defect	2	1	2	1
Gold (Au) Epoxy	**Defect**	4	2	2	2
	No Defect	2	1	2	1
Carbon (C) Paint	**Defect**	4	2		
	No Defect	2	1		
Silver (Ag) Paint	**Defect**	4	2		
	No Defect	2	1		
Nickel (Ni) Paint	**No Defect**		2		

3. To determine the electrochemical characteristics (coating capacitance, pore resistance, impedance, etc.) of samples with and without defects.

4. To determine the correlation between electrochemical characteristics and the severity of corrosion in coated specimens.

5. To determine coating integrity, including de-adhesion, using principles of ellipsometry to verify electrochemical results.

6. To perform X-ray Photoelectron Spectroscopy (XPS) and Scanning Auger Microprobe (SAM) testing on samples to correlate interfacial chemistry with EIS and ellipsometry.

7. To prepare a report.

ACTIVITY:

The functions performed in order to accomplish this task include:

(1) The acquisition of certified Al 2024-T3 sample material.

(2) The machining of Al 2024-T3 into 1 and 2 square inch samples for electrochemical testing according to ASTM G106-09.

(3) The application of aircraft coating waterborne epoxy and epoxy polyamide according to military specifications Mil-P-85582 and Mil-P-23377, respectively.

(4) The acquisition of Gold (Au), Silver (Ag), Carbon (C), and Nickel (Ni) paint as electrode materials.

(5) The design and construction of a paintable electrode structure with Gold (Au), Silver (Ag), Carbon (C), and Nickel (Ni) conductive paints.

(6) The performance testing of Electrochemical Impedance Spectroscopy on painted electrode Al 2024-T3 samples.

(7) Verification of electrochemical results obtained from the painted electrodes using the EG&G PAR Flat Cell electrochemical cell.

(8) The performance of ellipsometry and potentiodynamic scans on samples to verify AC Impedance results and to indicate possible de-adhesion of the coating from the substrate.

(9) The performance of salt spray testing on samples to determine the ability of the conductive paint electrodes to track the corrosion process.

(10) The performance of XPS on test samples to correlate interfacial chemistry with electrochemical results. Not completed due to use of additional electrode specimens and late completion of salt spray tests. This work is on-going.

(11) The preparation of the final report and analysis of the results.

EXPERIMENTAL:

1. Al 2024-T3 Sample Preparation

A 3' x 4' x 1/32" sheet of guaranteed Al 2024-T3 was obtained from C-S Metals Service, Inc. The sheet was then professionally machined into sixty (60) rectangular samples (2"x2"x1/32") by Bill Adams of Adams Machine and Tool Shop. The sixty (60) samples were then sent to Courtaulds Aerospace in Berkeley, CA where the samples were prepared with the following materials and their specifications:

(30)	*Epoxy Polyamide Primer*	*Mil-P-23377*
	Urethane Topcoat	*Mil-C-83286*
(30)	*Waterborne Epoxy Primer*	*Mil-P-85582*
	Urethane Topcoat	*Mil-C-83286*

Seven (7) of the waterborne epoxy primer and five (5) of the epoxy polyamide primer 2" x 2" samples were each cut into four (4) 1" x 1" sections by Adams Machine and Tool Shop. This was done to accommodate more extensive testing of the painted electrodes. Furthermore, it maximized the test area of each sample.

- *A coated sample (electrode-less) is displayed in Figure 17.*

2. Conductive Paint Electrodes

Cleaning of the Coated Surface

The coated surface of each sample was rinsed with isopropyl alcohol (IPA) from a rinse bottle while held with tweezers in a lower corner. Rinses were performed until no surface streaks or spots were observed. The panels were handled only with clean gloves and tweezers during and after cleaning.

Masking of the Coated Surface

An outer frame of dimensions 1" x 1" was constructed of 3M #658 Post-it correction tape. A square with sides of 17/32" was cut out of the middle of this frame with sides parallel to the outside sides. From a different piece of the 3M tape another square piece was cut with sides measuring 15/32". The smaller square was placed on the painted Al panels with the outer frame around it so that the gap between the two masking elements was about 1/16" inch all around as shown below.

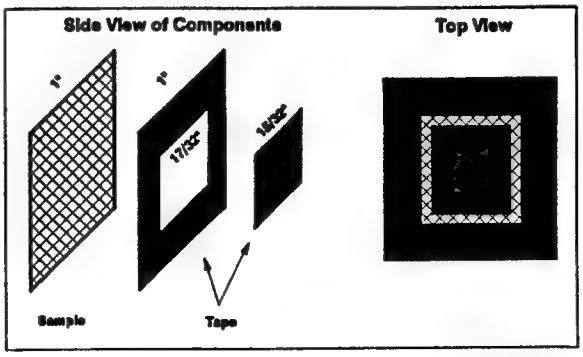

Template used to apply conductive paint to the aircraft metal/coating system.

Application of Electrodes

The electrodes were formed by painting conductive paints onto the panels through the gap in the tape mask using a fingernail polish brush, which was cleaned with IPA when switching to another paint. The conductive paint, epoxy materials, and curing conditions used are listed in Table 3. The painted electrodes were allowed to dry at room temperature for at least thirty (30) minutes and then the frame was removed.

Application of Wires to the Electrode and Sample

The wires were stripped of their insulation and the exposed metal was cleaned with IPA. One wire was attached to the electrode by laying it into a pool of the conductive silver 2-part epoxy listed in the table below in contact with the epoxy coating on the top side. After curing at room temperature for thirty minutes, the samples were placed in the oven to cure at 50°C for 20 hours. 3M 1838 B/A two part epoxy adhesive was then applied on the surface of the silver epoxy used to bond the wire for the purpose of adding additional strength and protection to the bond.

Table 3. *Specifications for application of electrodes.*

Material	Supplier	Item #	Thinner Used	Cure Temperature (C)	Cure Time (hrs)
2-part Gold Epoxy	Epoxy Technology Inc.	H81E	Yes	80	2.5
2-part Gold Epoxy	Epoxy Technology Inc.	H81E	Yes	50	20
Silver Paint	Creative Materials	102-05F	No	50	20
2-part Silver Epoxy	TRA-CON	BA-2902	Yes	50	20
Carbon Paint	Creative Materials	104-18	No	50	20
2-part Nickel Epoxy	TRA-CON	BA-2701	Yes	Unsuited for electrode application	
Nickel Paint	Creative Materials	115-05	No	50	20
Thinner	Creative Materials	113-12			

Application of Glyptal to Samples
Glyptal was applied to all exposed aluminum surfaces including edges and the backside of each sample according to ASTM D-609. Glyptal is meant to provide a coating to the bare aluminum and to prevent the aluminum from absorbing any water through the sides and back of the sample. Therefore, water can only be absorbed through the coating representing the case of an aircraft coating.

Scribing of Samples
Several batches of electrodes were scribed in order to perform salt fog testing and corrosion testing. Scribing was performed according to ASTM D 1654-79a. Two one (1) centimeter lengths inside the electrode area were scribed in the shape of an "X" with the aluminum substrate being exposed.

The scope of work for the development of the electrodes included testing of several conductive paints. Gold epoxy was the obvious first choice due to its extremely high electrical conductivity. Silver, carbon, and nickel epoxies were chosen as low cost alternatives to the gold epoxy. The following paints and epoxies have been utilized for the electrode sensors:

Gold Epoxy
The gold epoxy used as a painted electrode was the EPO-TEK H81E from Epoxy Technology, Inc. The EPO-TEK H81E is a two component, gold filled epoxy. The paint is a 100% solids (solventless) and will not outgass. In addition, the gold paint has high electrical conductivity resulting in low interfacial impedance between the gold and the coating. A drawback of the gold paint is the price.

Silver Paint
The silver paint used for painted electrodes is the 102-05F electrically conductive ink from Creative Materials, Inc. The 102-05F is a one part 85% silver paint. The paint has high solvent resistance and has excellent adhesion and is resistant to scratching and abrasion. The silver paint is a lower cost alternative to the gold epoxy, but might not prove sufficiently corrosion resistant, it was feared.

Carbon Paint
The carbon paint used for painted electrodes is the 104-18 electrically conductive ink from Creative Materials, Inc. The 104-18 is a one part 85% carbon paint. Even though the electrical conductivity of the carbon is less than that of the gold paint, the carbon paint still has a much greater conductivity as compared to the coating to which it will be applied. Results are expected to be similar to the gold paint electrodes. Carbon conductive paint is the most cost effective alternative to the gold and silver paints.

Nickel Paint
The nickel paint used for painted electrodes is the 115-05 electrically conductive ink from Creative Materials, Inc. The 115-05 is inexpensive and offers high conductivity. Furthermore, the nickel paint's corrosion resistance is greater than that of the silver paint and its abrasion resistance is greater than the carbon paint.

- *Typical coated samples with painted electrodes (Gold, Silver, and Carbon) are displayed in Figures 18, 19, and 20.*

3. Electrochemical Testing

AC Impedance Technique

Electrochemical Impedance Spectroscopy was performed on the machined samples using the EG&G Princeton Applied Research (PAR) Potentiostat Model 273. An EG&G PAR Lock-in Amplifier Model 5210 was used in order to generate the alternating current waveform. EG&G PAR Model 398 version 1.10 Electrochemical Impedance software was used.

The EG&G PAR K0235 Flat Cell electrochemical cell was used to verify results obtained from the painted electrodes. A 250 mL .05 Molar Na_2SO_4 solution (pH = 6.05) was used as the electrolyte. The corrosion cell requires the use of an electrolyte and a counter electrode. Three electrical connections were made using the corrosion cell. A working electrode was connected to the backside of the sample. The reference electrode was connected to a Silver/Silver Chloride electrode to measure the current. The third connection was for the counter electrode.

Painted electrodes were tested without the use of an electrochemical corrosion cell. The electrodes were connected directly to the potentiostat. The working electrode was connected to the metal backside of the sample. The reference electrode was electrically connected to the painted electrode. The counter electrode was left unconnected.

- *The electrochemical testing set-up is displayed in Figure 21.*
- *The EG&G PAR Model K0235 Flat Cell electrochemical cell is displayed in Figure 22.*

DC Potentiodynamic Scans

The EG&G PAR Model K47 Corrosion Cell System was used to perform potentiodynamic scans according to ASTM G5-94 on the samples in order to calculate corrosion rates. A .05 Molar Na_2SO_4 solution was used as the electrolyte. Prior to testing, each sample was thoroughly rinsed with de-ionized water and allowed to dry. The sample was then immersed completely in the electrolyte and electrically connected as the working electrode. A reference electrode (Potassium Chloride) was positioned next to the sample and connected to the potentiostat. Two graphite rods immersed in the electrolyte acted as the counter electrodes. Using the EG&G PAR Model 352 SoftCorr II Corrosion Measurement and Analysis Software, DC current was then sent through the sample to induce corrosion. The corrosion rate and protection potential were then calculated from the resulting data.

- *The three-electrode EG&G PAR Model K47 Corrosion Cell is displayed in Figure 23.*
- *A close-up of a sample immersed in the Model K47 Corrosion Cell is displayed in Figure 24.*

4. Ellipsometry

Ellipsometry was conducted using the Gaertner Scientific Model L119x Ellipsometer using a 4 mW Helium-Neon laser with a wavelength of 6238 Å. Prior to being tested, each sample was thoroughly rinsed with de-ionized water and allowed to dry. A flat panel holder with four restraining clamps was used to hold an individual sample. The laser light passed through the quarter-wave plate and reflected off the sample. The reflected light then entered the photocell. The photocell was then adjusted to allow the maximum amount of light through. The sample was adjusted on the flat panel holder until the photodetector measured an intensity of 2 with the range set to 6. Gaertner Scientific GS-SC4A L104 software package was used to automatically control the photocell and determine the null point. The index of refraction, coefficient of extinction, Psi, and Delta were then calculated. Multiple measurements (5-10) were taken for each sample to obtain more precise results.

• *The ellipsometrical testing set-up is displayed in Figures 25 and 26.*

5. Salt Fog Testing

Salt spray testing was conducted using the Singleton Corporation SCCH Corrosion Test Cabinet Model 20. A 5% NaCl solution at 99°F was used. Salt fog testing was conducted according to ASTM B117. Samples were placed in a specimen holder capable of holding twenty samples. Testing was interrupted periodically to perform AC Impedance tests on the samples to track the corrosion process. When removed from the salt fog chamber, each sample was rinsed with distilled water, dried with a nitrogen stream, and measured within twenty (20) minutes or less after removal. The experimental procedure was changed at exposure times greater than 674 hours due to premature blistering of the glyptal on the backside of the coupons. When removed from the exposure chamber, samples were rinsed and dried off with nitrogen. Each sample was allowed to dry for at least thirty (30) minutes. Measurements were then taken and showed no discontinuities between the low and the high frequency range data sets.

6. XPS Characterization

XPS characterization of bare metal Al 2024-T3 and the urethane topcoat of the coated samples was conducted using the Surface Science Instruments SSX-100 system with a torodial crystal monochromatized Al x-ray source. The sample is mounted on a rotatable sample holder. A base analysis chamber pressure of less than 3×10^{-9} Torr insures that superficially adsorbed vapors on surfaces are removed and reduces the possibility of contaminant vapor adsorption on surfaces during analysis. The analysis chamber is principally pumped by a 240 l/s ion

pump with an auxiliary titanium sublimation getter pump which can handle a relatively large vapor output. A sample introduction chamber which is separately pumped by a 50 l/s turbomolecular pump prevents exposure of the analysis chamber to heavy gas loads upon the introduction of new samples. After the pressure in the sample introduction chamber is brought below 1×10^{-6} Torr, the sample is passed into a sample preparation chamber which is pumped by a 120 l/s ion pump. The base pressure in this chamber is less than 3×10^{-9} Torr and it is not allowed to rise above 1×10^{-6} Torr during the introduction of a sample into this chamber. When samples are next introduced into the analysis chamber, the pressure is not allowed to rise above 4×10^{-7} Torr. This sample introduction process is very effective in eliminating contamination of the vacuum system and the cross-contamination of samples.

- *XPS setup is displayed in Figures 27 and 28.*

7. SAM Characterization

Samples are introduced through a sample introduction chamber equipped with a 170l/s turbomolecular pump for fast pump-down times. The analysis chamber is pumped by a 200l/s ion pump and a 1600l/s titanium sublimation pump. The ultimate analysis chamber base pressure is $< 10^{-7}$ Pa or $< 10^{-9}$ Torr. In practice, the pressure is usually $< 5 \times 10^{-9}$ Torr. The electron optical column is pumped by a separate 32l/s ion pump. The system is also equipped with a differentially pumped ion gun to enable depth profiles to depths as great as 2μm, without straining the analyzer chamber ion pump or introducing backstreaming pump contamination.

- *SAM setup is displayed in Figures 29 and 30.*

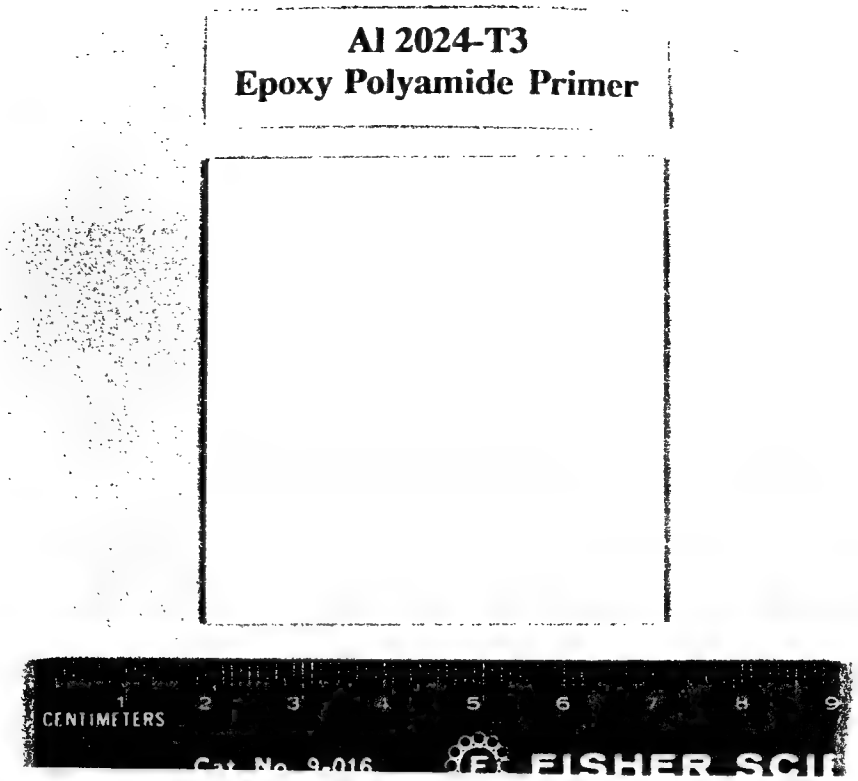

Figure 17. *Aircraft aluminum 2024-T3 sample (electrode-less) with MIL-P-85582 epoxy polyamide primer and MIL-C-83286 urethane topcoat.*

Figure 18. *Aircraft aluminum 2024-T3 sample with applied gold conductive epoxy electrode enabling two-electrode AC Impedance testing.*

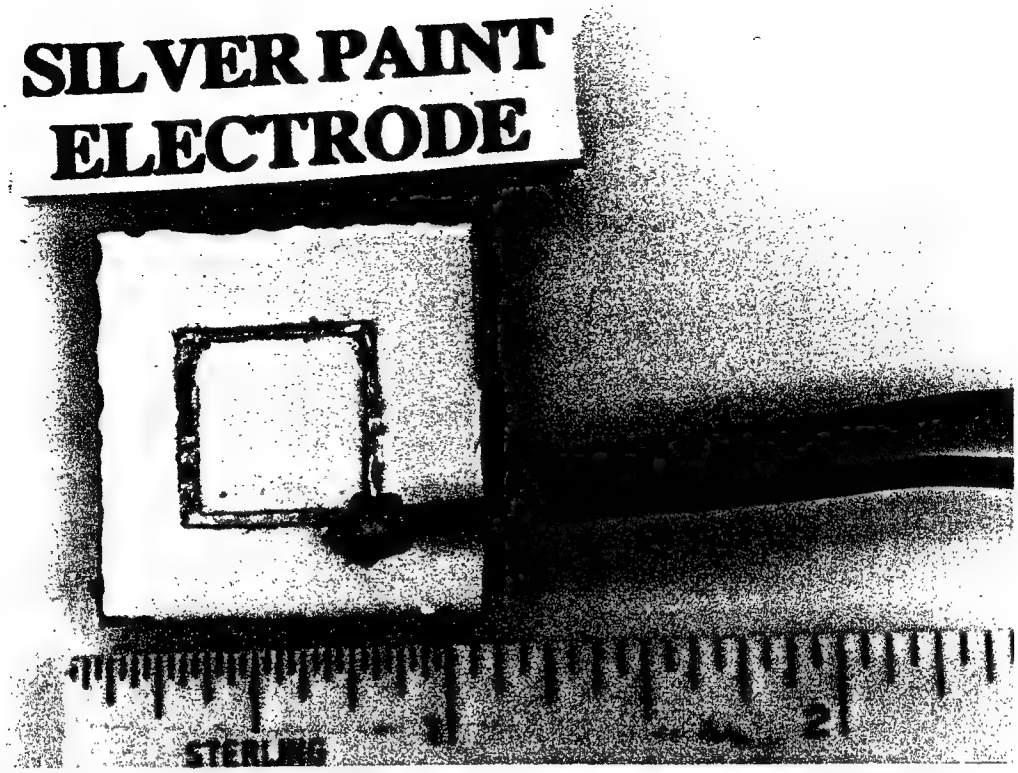

Figure 19. *Aircraft aluminum 2024-T3 sample with applied silver conductive paint electrode enabling two-electrode AC Impedance testing.*

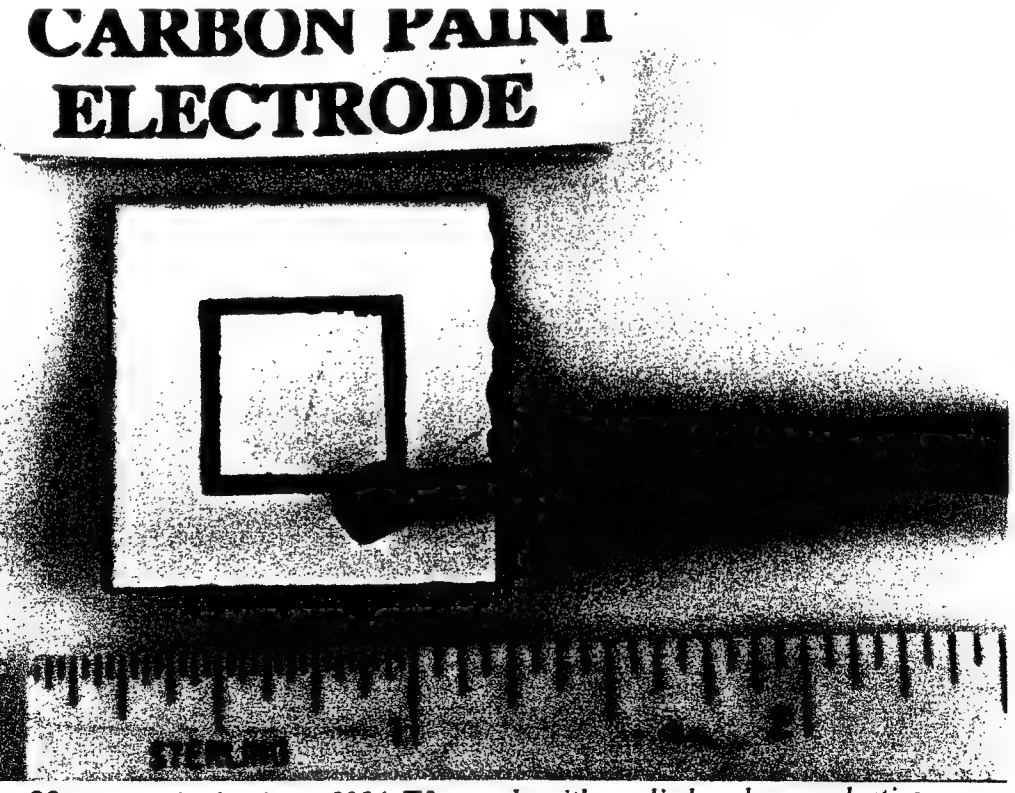

Figure 20. *Aircraft aluminum 2024-T3 sample with applied carbon conductive paint electrode enabling two-electrode AC Impedance testing.*

Figure 21. *Electrochemical testing set-up (computer, potentiostat, and lock-in amplifier).*

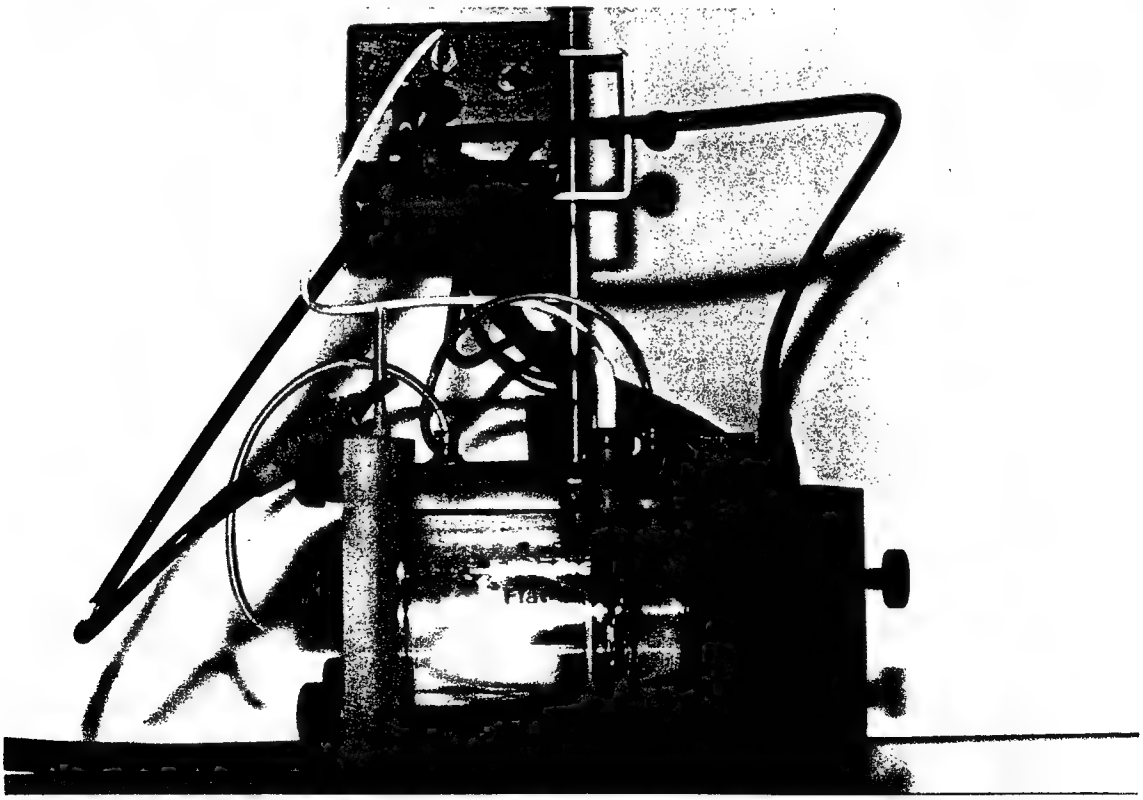

Figure 22. *EG&G PAR Model K0235 Flat Cell electrochemical corrosion cell permitting conventional three-electrode AC Impedance testing.*

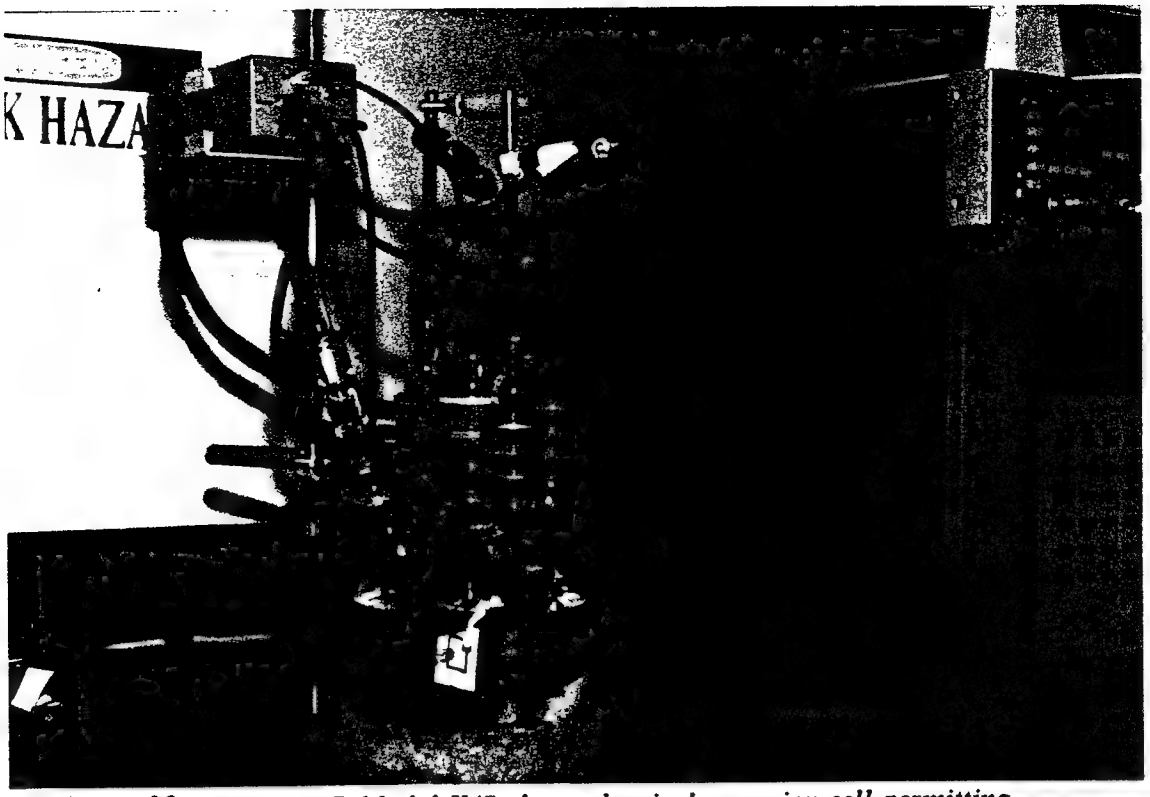

Figure 23. *EG&G PAR Model K47 electrochemical corrosion cell permitting conventional three-electrode AC Impedance testing.*

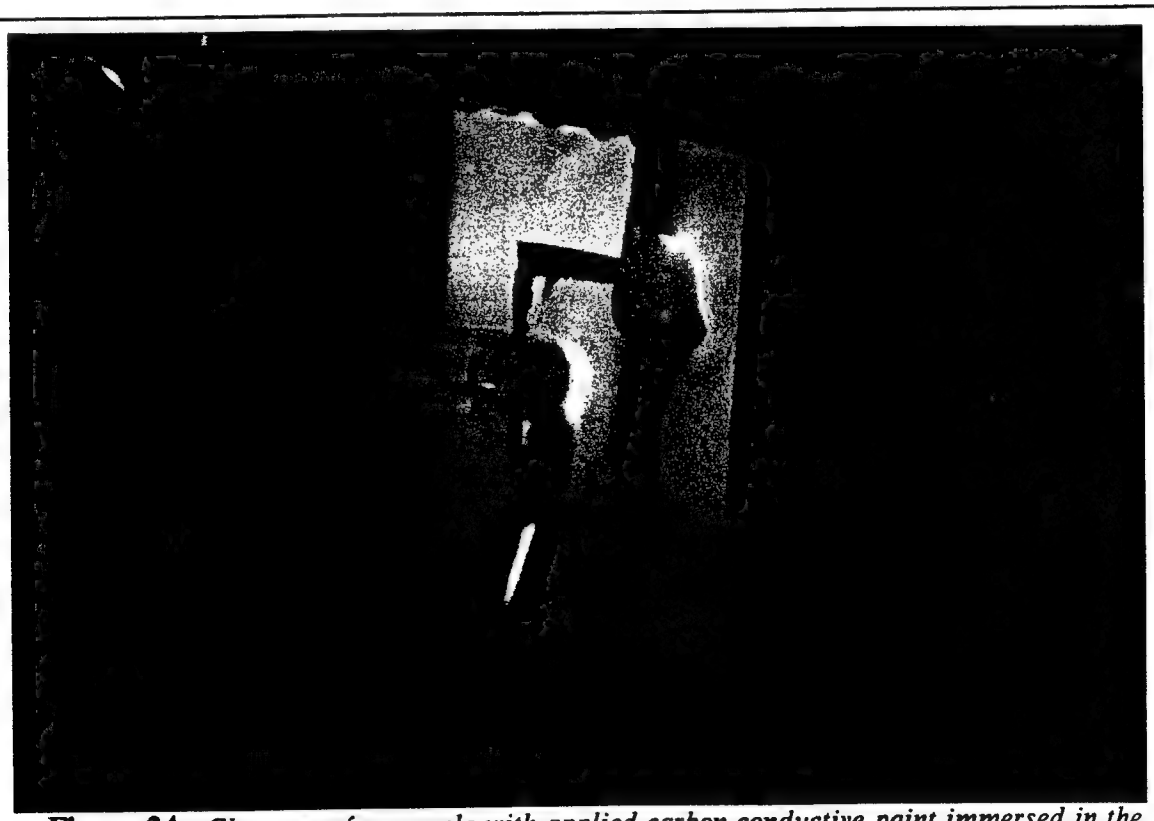

Figure 24. *Close-up of a sample with applied carbon conductive paint immersed in the EG&G PAR Model K47 electrochemical corrosion cell. The reference electrode with a salt bridge at the tip allows selective ions from electrolyte to be measured.*

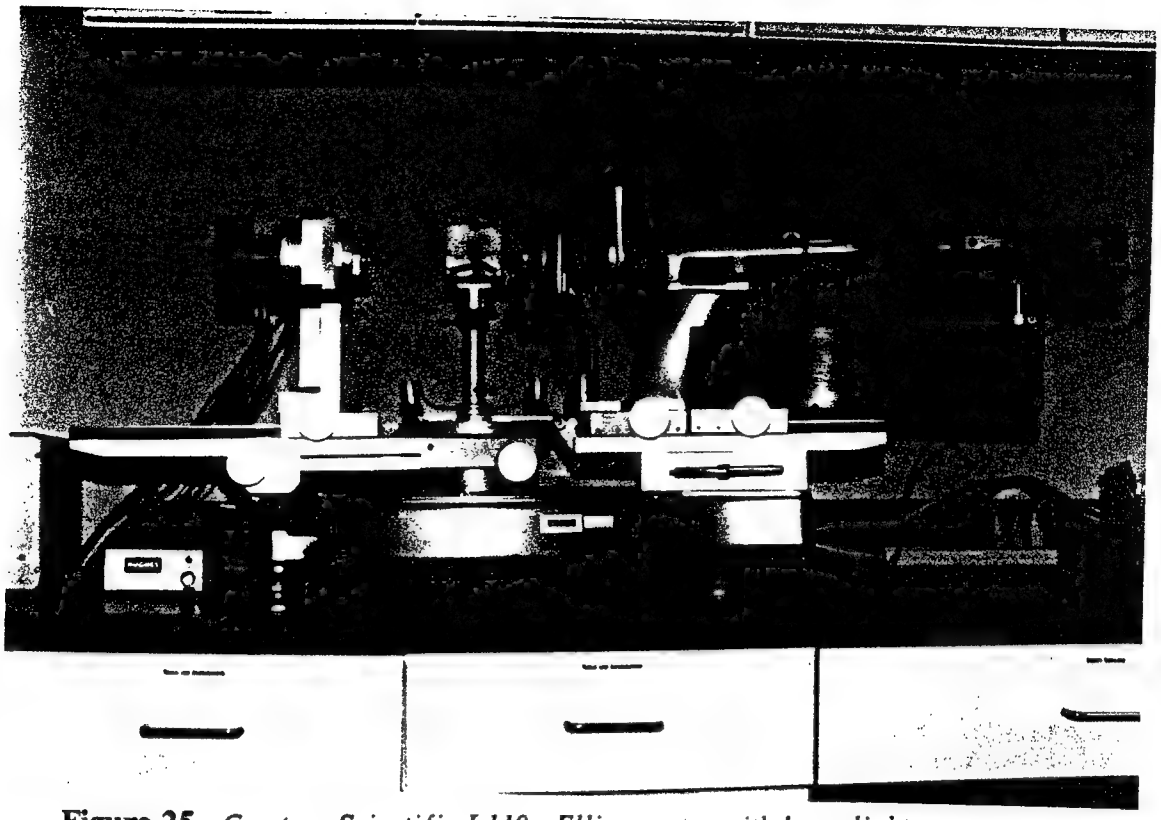

Figure 25. *Gaertner Scientific L119x Ellipsometer with laser light source.*

Figure 26. *Supporting equipment for the ellipsometer including photocell, electrical chassis box, and computer.*

Figure 27. *XPS setup - Surface Science Instruments SSX-100 System with related electronics.*

Figure 28. *XPS setup - analytical chamber of the Surface Science Instruments SSX-100 System.*

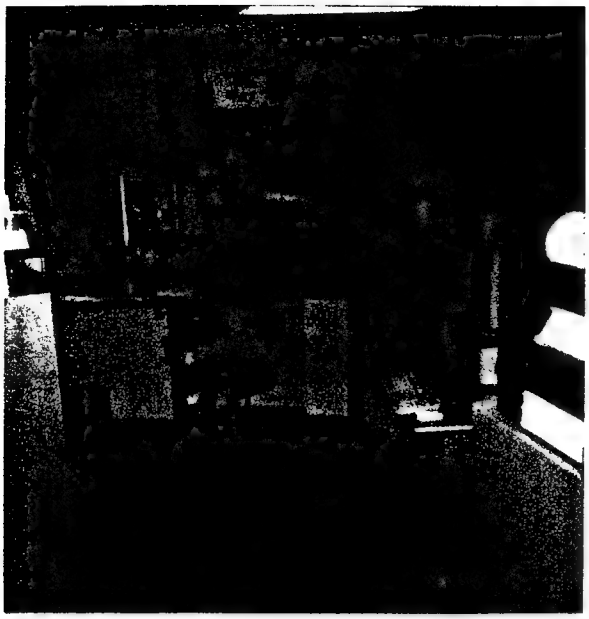

Figure 29. *SAM setup - JEOL Auger Microprobe JAMP-10S with related electronics.*

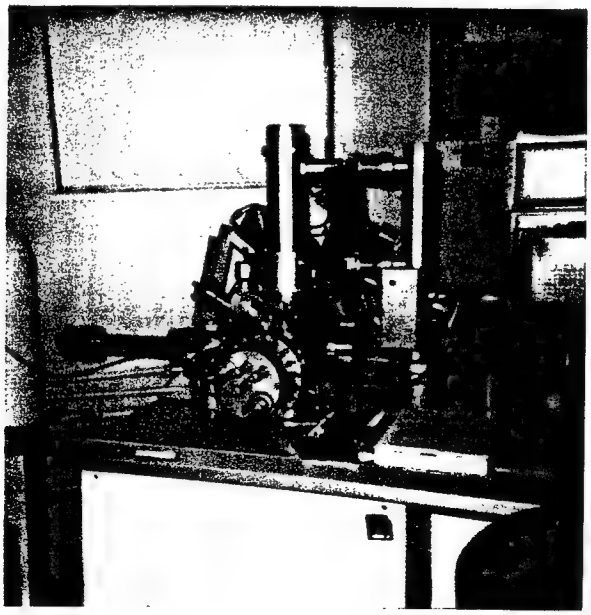

Figure 30. *SAM setup - Analysis vacuum chamber of the JEOL Auger Microprobe JAMP-10S*

RESULTS AND DISCUSSION:

Several types of analyses were performed in order to characterize the AC Impedance spectra that were obtained. First, the aluminum samples were prepared to simulate aircraft metal/coating systems. Testing was then performed to characterize the virgin samples. Initial testing was followed by design of electrode sensors capable of obtaining impedance spectrum. Samples (with and without electrodes) were tested using electrochemistry, ellipsometry, salt spray and immersion testing, and X-ray Photoelectron Spectroscopy to correlate and verify results obtained using the AC Impedance technique.

FABRICATION OF TEST SAMPLES

In an effort to provide a smooth transition from laboratory results to field operation of the AC Impedance technique, Al 2024 samples were coated according to military specifications in order to accurately simulate aircraft metal/coating systems. Phase I testing included aluminum 2024-T3 coated with MIL-P-85582 waterborne epoxy and MIL-C-83286 urethane topcoat and aluminum 2024-T3 coated with MIL-P-23377 epoxy polyamide and MIL-C-83286 urethane topcoat. These two metal/coating systems (Figure 31) are currently in use by the Air Force. An oxide is present on the aluminum substrate which provides natural protection from corrosion.

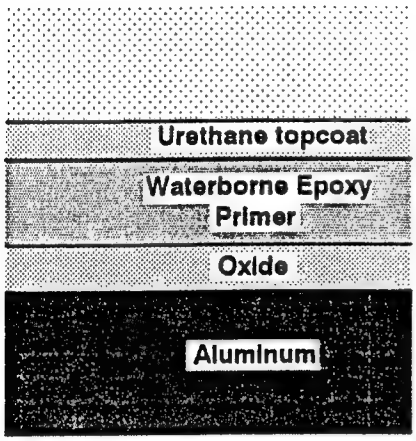

Mil-C-83286 Urethane topcoat
Mil-P-85582 Waterborne epoxy primer

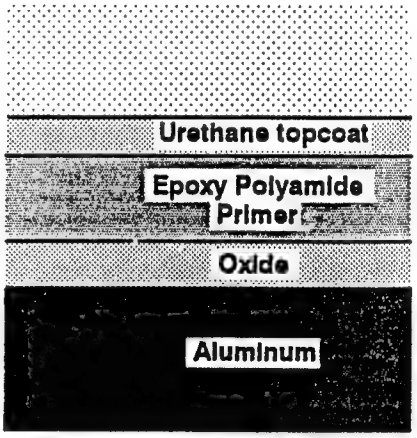

Mil-C-83286 Urethane topcoat
Mil-P-23377 Epoxy polyamide primer

Figure 31. *Aircraft metal/coating systems used for Phase I research.*

INITIAL TESTING OF SAMPLES

After being coated, two samples (one with waterborne epoxy primer and the other with epoxy polyamide primer) were photomicrographed (Figure 32) in order to analyze the appearance of the coating surface. Both specimens were very uniform in appearance, even though several small defects were documented on each specimen. This was verified with the ellipsometer, where it was determined that both metal/coating systems displayed identical refractive indices at various locations on the sample. This was anticipated, since both have an identical urethane topcoat. The sample with the waterborne epoxy primer was uniformly rough and patterned as shown. The surface is not entirely smooth (free of defects) but is still representative of the typical surface on aircraft.

(a) Al 2024 sample coated with the waterborne epoxy primer

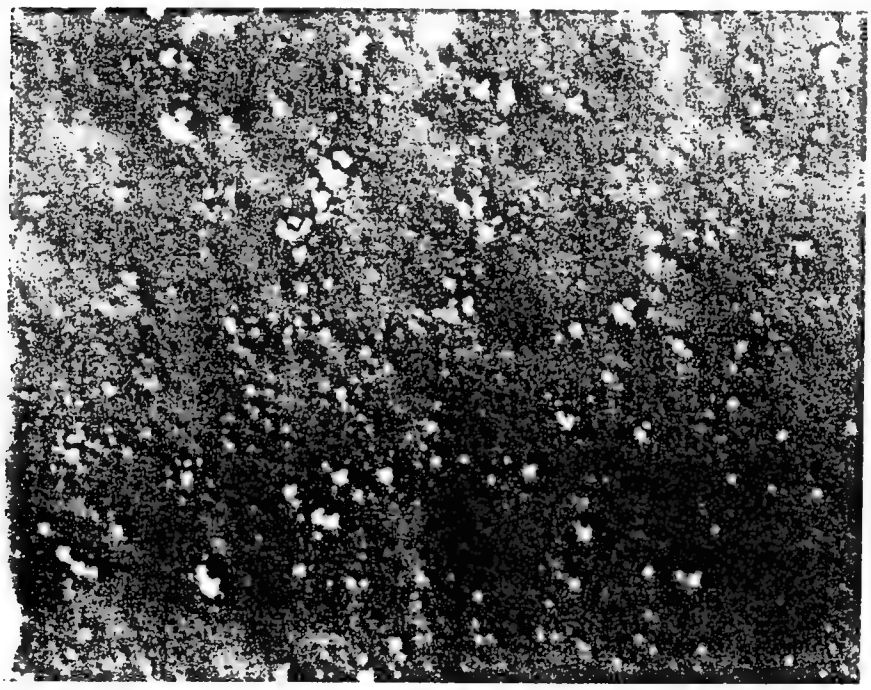

(b) Al 2024 sample coated with the epoxy polyamide primer

Figure 32. *Photomicrographs at 50X of aircraft aluminum 2024-T3 samples coated with (a) waterborne epoxy primer and (b) epoxy polyamide primer.*

X-ray Photoelectron Spectroscopy was performed in order to characterize the elemental species present in the aluminum substrate (Figure 33 and Table 4). The quantity of oxygen is consistent with the oxide of the hydrated species being primarily MgO and secondarily Al_2O_3. Little $Mg(OH)_2$, AlOOH, or $Al(OH)_3$ can be present since these would imply higher oxygen concentrations than found. The oxide is highly enriched in Mg relative to Al when compared to their ratio in the bulk composition. Cu, which is prevalent, or more so, than Mg in the bulk, is barely detectable on the surface.

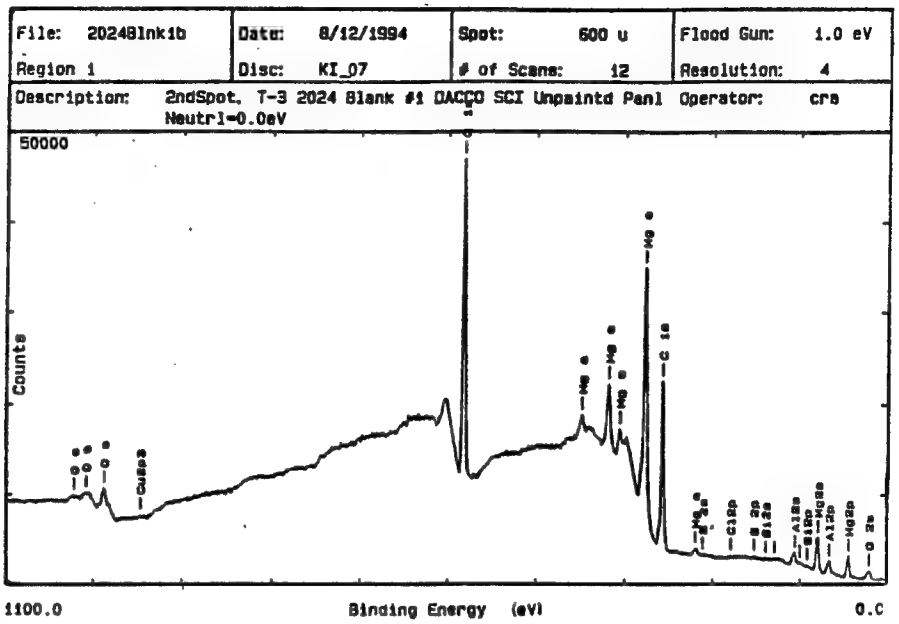

Figure 33. *X-ray Photoelectron Spectroscopy of an unpainted Al 2024-T3 specimen.*

Table 4. *XPS of an unpainted Al 2024-T3 specimen. The table compares those concentrations with the bulk composition in atomic percent after converting the Al 2024 alloy composition from weight percent.*

Specimen Element	Bulk wt. %	Bulk at. %	Surface Spot 1	Surface Spot 2
Al	94.70 - 90.75	96.70 - 94.53	9.20	8.62
Cu	3.8 - 4.9	1.72 - 2.08	0.08	0.02
Mg	1.2 - 1.8	1.42 - 2.00	17.16	15.07
Mn	0.30 - 0.9	0.16 - 0.44		
Fe	< 0.5	< 0.24		
Si	< 0.5	< 0.48	0.28	0.32
Zn	< 0.25	< 0.10		
Ti	< 0.15	< 0.08		
Cr	< 0.10	< 0.05		
C			40.63	42.56
O			31.91	32.98
S			0.39	0.29
Cl			0.16	0.14
Na				0.20

Several samples underwent AC impedance testing in a conventional three-electrode corrosion cell to obtain initial impedance spectra (Figure 34). Analysis of the spectra revealed that the aluminum 2024-T3 coated with the waterborne epoxy primer displayed larger impedance values than the epoxy polyamide primer at all frequencies. This was confirmed from analysis of the Nyquist plot of both primers where it is evident that the waterborne epoxy exhibits larger real and imaginary impedance values than the epoxy polyamide. This preliminarily indicated that the samples coated with waterborne epoxy primer had a higher resistance, were more thickly coated, or absorbed less water than those coated with the epoxy polyamide primer. A thicker coating and less water absorption are both likely to correlate with an increased corrosion resistance.

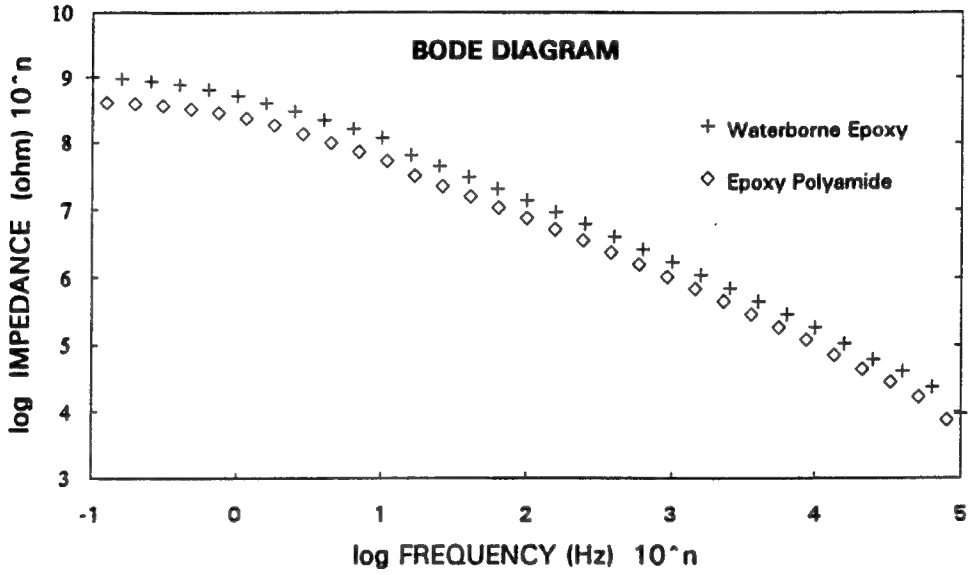

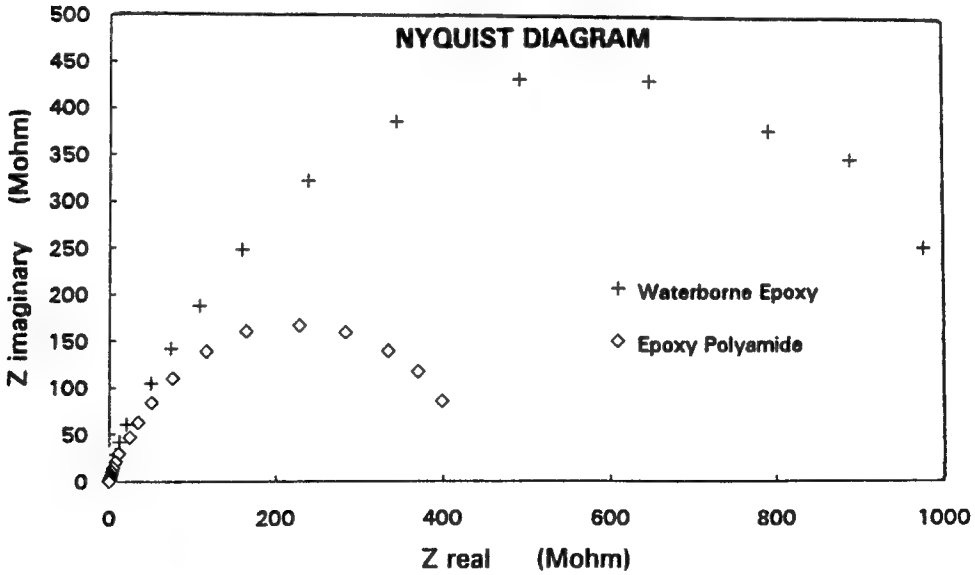

Figure 34. *Bode and Nyquist diagrams from initial testing of aircraft aluminum 2024-T3 samples coated with waterborne epoxy and epoxy polyamide primers.*

DESIGN AND FABRICATION OF ELECTRODES

The preliminary testing indicated that the AC impedance technique was capable of obtaining the impedance spectrum for both aircraft metal/coating systems tested. Initial testing was accomplished using a conventional three-electrode corrosion cell set-up. This required the use of a counter electrode and an electrolyte (250 mL of .05M Na_2SO_4). Conventional three-electrode testing makes in-situ field testing extremely difficult and in most cases infeasible to perform.

Prototype electrode sensors were designed by DACCO SCI, INC in the Phase I effort to make in-situ testing more feasible. These electrode sensors are capable of detecting the impedance spectra of aircraft metal/coating systems using a two-electrode approach. Laboratory versions of the proposed electrodes (Figure 35) have a conductive epoxy paint (gold, silver, nickel, or carbon) deposited onto the coating and a contact to the backside of the coupon. The use of a painted electrode on the surface of the metal/coating system eliminates the need for a counter electrode since the impedance of the paint is much less than that of the coating. The conductive paint is applied directly to the surface of the coating, resulting in the paint/coating interface having a much lower interfacial impedance as compared to the metal/coating interface. This allows the entire surface of the conductive paint to be utilized and results in a valid two-electrode approach. This two-electrode method enables in-situ real-time analysis of an aircraft metal/coating system, previously unavailable. Furthermore, it has been determined that the contact of the conductive paint electrode with the coating does not accelerate or initiate corrosion of the coating at the contact point. Results from the two-electrode approach have excellent overlays with conventional three-electrode results. These electrode sensors represent an opportunity to develop an uncomplicated straightforward sensor capable of quickly assessing the integrity of any aircraft metal/coating system.

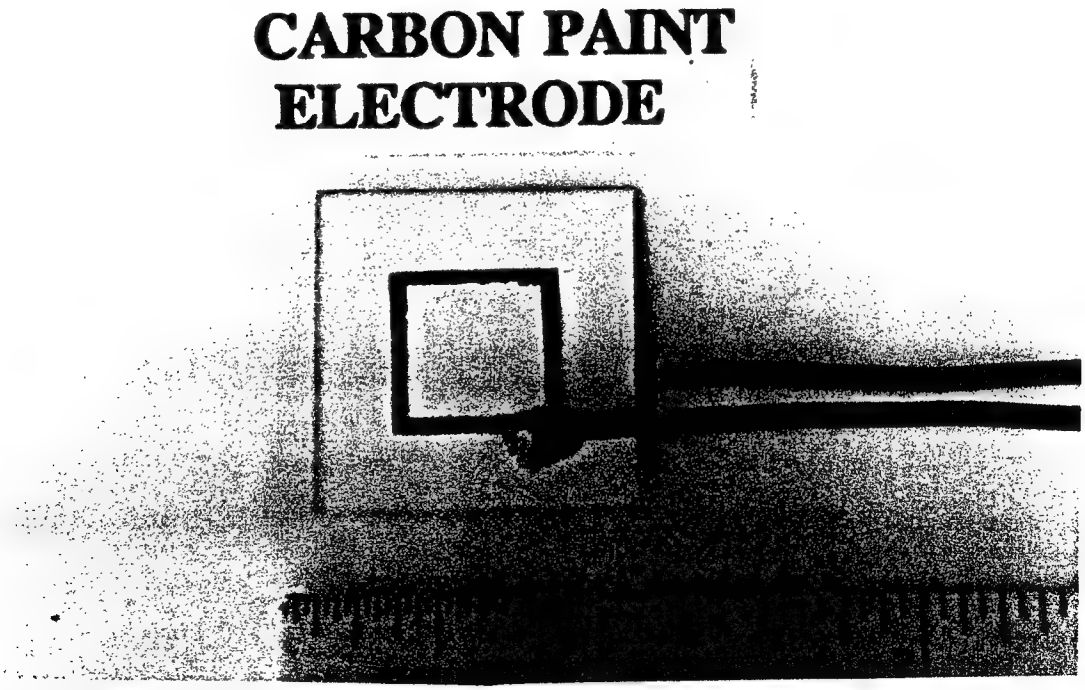

Figure 35. *Conductive paint (carbon) electrode deposited onto waterborne epoxy sample enabling two-electrode AC Impedance testing by eliminating the need for a counter electrode.*

Initial fabrication of the electrode sensors met with little success. The first template designed incorporated the use of an aluminum screen through which the paint was to be applied. Due to the consistency of the conductive paints, much of the paint adhered to the screen and not to the coating. This technique was abandoned for a more practical approach using a low-adhesive strength tape to lay the pattern of the grid. This technique proved to be simpler in design and allowed for easier application of the paint, provided the tape is removed before the epoxy paints are dried extensively.

Gold epoxy was the obvious first choice for use as an electrode. Gold has excellent electrical conductivity and has a high resistance to corrosion. The major drawback of the gold epoxy is the cost. Carbon paint was used to provide a low cost alternative to the gold paint. Even though the electrical conductivity is less than that of the gold paint, the carbon paint still has a much greater conductivity compared to the coating it will be applied to.

Silver and nickel conductive epoxies were added to the scope of testing to provide more low-cost alternatives to the gold epoxy since there was concern that the carbon paint might not give accurate results due its low electrical conductivity and suspected low abrasion resistance. The nickel paint, in addition to its high electrical conductivity, has excellent resistance to abrasion. The values for the measured electrical conductivity of the deposited epoxy paint electrodes are shown in Table 5.

Table 5. *Current resistance of painted electrodes taken from opposite corners of the deposited electrode grid.*

Electrode Paint	Cure Temp. (C)	Resistance (Ohms)
Gold (Au)	50	4.5
Gold (Au)	80	2
Silver (Ag)	50	.4
Nickel (Ni)	50	1
Carbon (C)	50	675

It was found that the conductivity of the gold epoxy increased with cure temperature as supported by the specification sheet sent with the epoxy. However, there was concern that elevated cure temperatures might adversely alter the integrity of the coating. Therefore, the lowest possible recommended cure temperature of 50°C was chosen for all the paints. The lowest possible cure temperature is also more practical for field application of the conductive paint electrodes.

Application of the conductive paint electrodes did not appear to alter the coating surface, with the exception of the gold epoxy paint, which subtly changed the appearance of the paint coating on both coating system types. This was verified both visually and with the ellipsometer, in which, no changes in the refractive index were observed after the application of the electrode.

AC IMPEDANCE TESTING

AC impedance testing was then conducted on the electrode sensors to quantify any differences in impedance spectra obtained previously from the three-electrode method. It was found that the impedance was much higher, approximately one order of magnitude for both primers, after the electrodes were applied to the coating (Figure 36). It was determined that the difference in the overlays was due to the curing of the painted electrodes on the specimen. The curing of the electrodes at 50°C for 20 hours evaporated all solvents and water that were located within the coating. In the time it took to get the samples back from being professionally coated, the samples had experienced an initial water uptake which was measured and quantified using the AC Impedance technique. The curing process increases the impedance of the coating and represents a reproducible baseline reference. It should be noted that the AC Impedance tests do not induce corrosion and these results are easily reproducible.

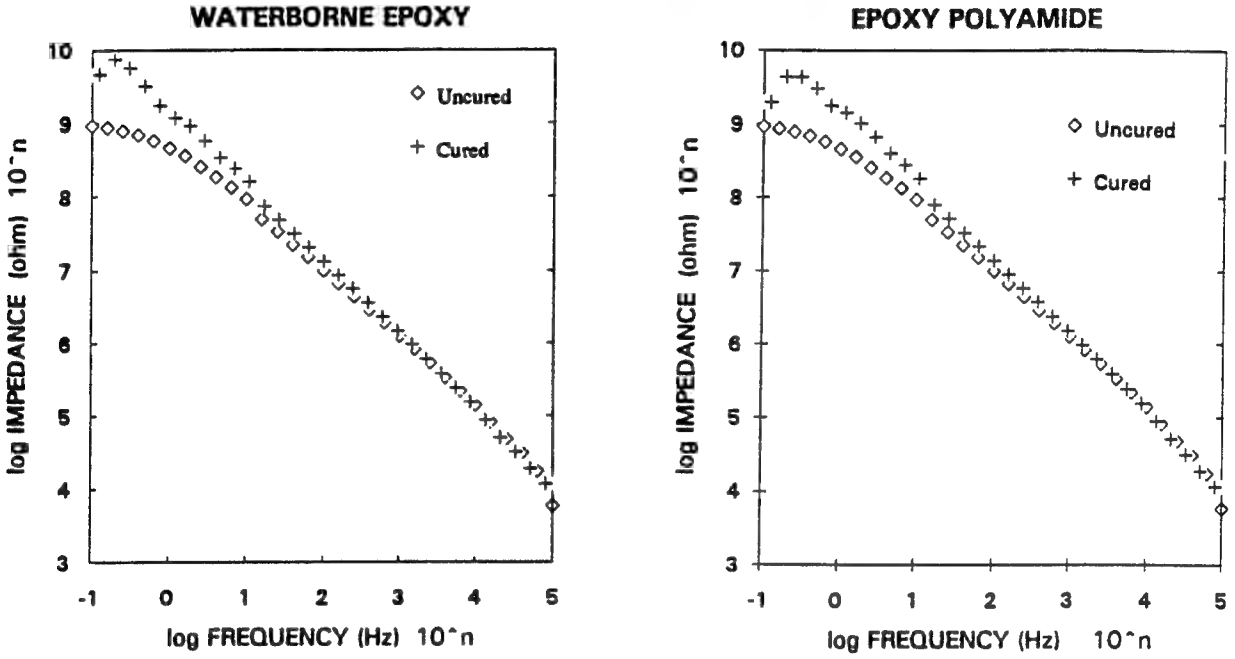

Figure 36. *Bode plots of impedance spectrum of cured and uncured electrode-less samples using the conventional three-electrode method. A .05M Na_2SO_4 solution was used as the electrolyte.*

Based on this information, AC impedance spectra were obtained for cured electrode-less samples using the three-electrode method and overlaid with the spectra for the conductive paint electrode sensors using the two-electrode approach (Figures 37 and 38). The gold, silver, and nickel conductive paint electrode results show a remarkable overlay with the three-electrode electrode-less spectrum. Some of the carbon electrodes had difficulty tracking the impedance spectrum of the baseline. These discrepancies in results for the carbon paint electrodes could be due to its lower electrical conductivity or to a process in which the graphite particles become surrounded and isolated by the epoxy polymer and results in a higher impedance than would be expected. The well behaved carbon electrode suggests that this may be a solvable problem. Variables such as the cure temperature, the starting viscosity, and the amount of paint applied could be adjusted to increase the electrical conductivity.

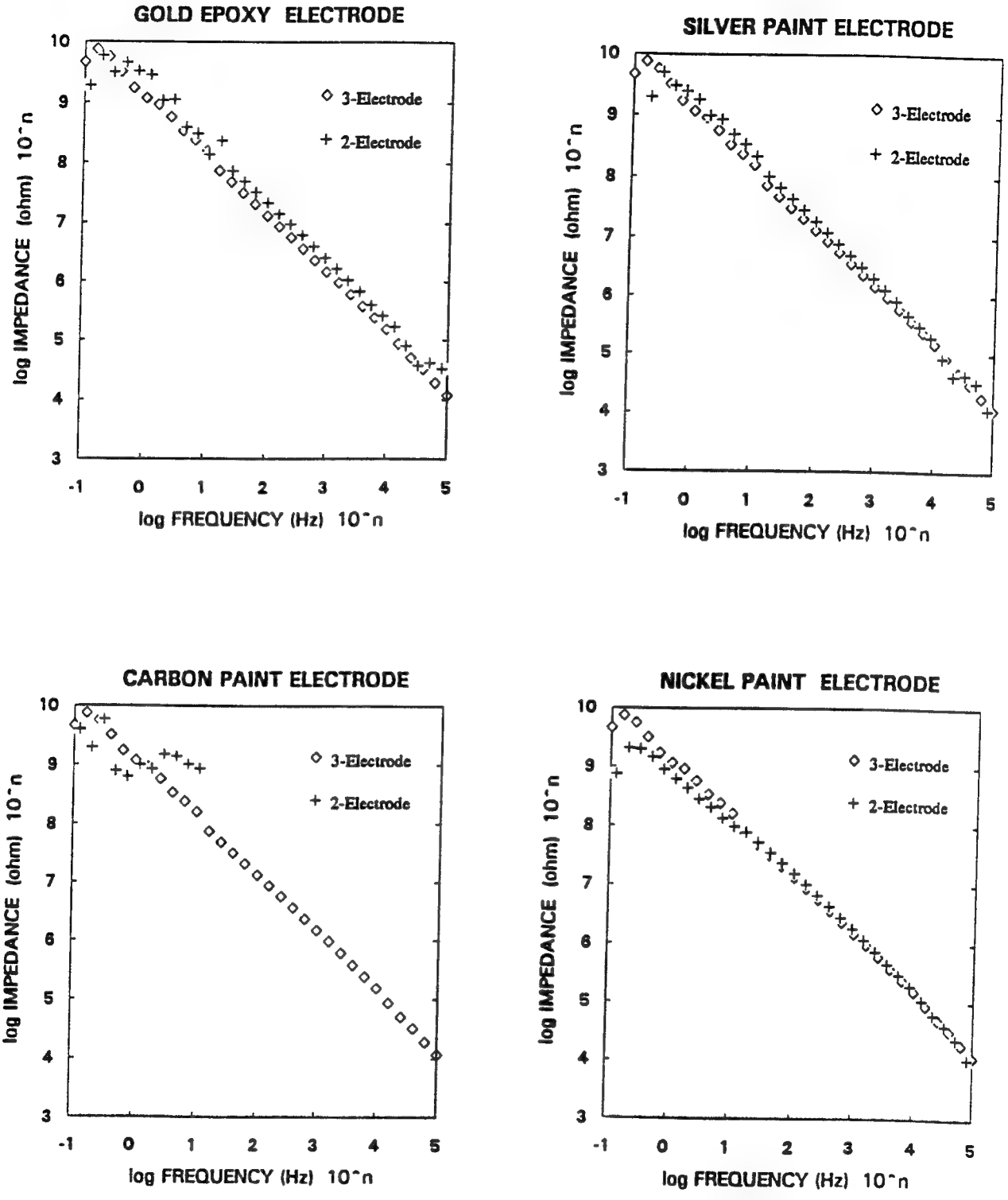

Figure 37. *Two-electrode impedance spectrum (Bode plots) for gold, silver, carbon, and nickel conductive epoxies on Al 2024-T3 coated with* ***waterborne epoxy*** *primer compared to conventional three-electrode results from an electrode-less sample.*

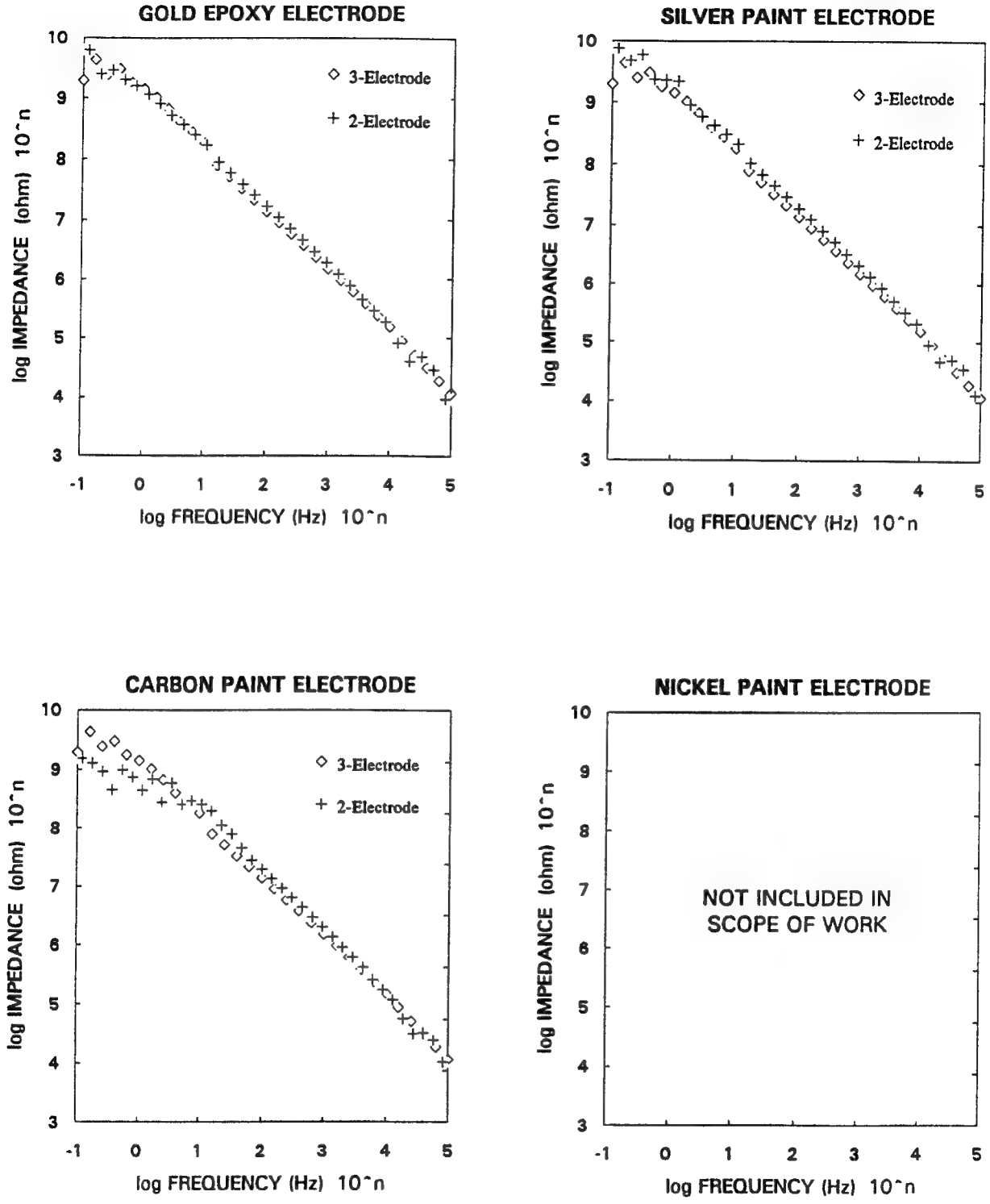

Figure 38. *Two-electrode impedance spectrum (Bode plots) for gold, silver, carbon, and nickel conductive epoxies on Al 2024-T3 coated with* ***epoxy polyamide*** *primer compared to conventional three-electrode results from an electrode-less sample.*

Due to the nature of the equivalent circuit model for the aircraft metal/coating system (see theory of ECM in Introduction), several variables exist to monitor coating performance including:

coating capacitance (C_c),
pore resistance (R_{po}), *and*
low-frequency impedance (Z_{if})

For the purposes of this testing it was found that the low-frequency impedance value obtained from the AC Impedance spectrum was the most optimal parameter for simply characterizing coating performance. Low-frequency values are easily discernible as the upper plateau of the spectrum, typically at frequencies less than 1 Hertz. Coating capacitance proved useful in measuring water uptake. However C_c proved to be less effective in the incubation and corrosion stage. Changes in this variable did not correlate well with visual observations. The second parameter, pore resistance, is a reflection of the amount of penetration by the electrolyte into the coating. This parameter like C_c did not track the corrosion process well after the water uptake stage. Throughout the entire corrosion process, the low-frequency impedance proved to be the best parameter in determining coating performance. Figure 39 is an overlay plot of the impedance spectrum from an immersion test of a painted steel specimen. Low-frequency impedance values trend downward indicating a predictable response from the low-frequency impedance in relation to the amount of corrosion. This correlated well with both visual and experimental observations throughout the Phase I testing. It can be seen in Figure 39 that the spectrum begins to converge in the intermediate frequencies and ultimately converge to the same high frequency values. Although it is possible to evaluate coating performance using either pore resistance or coating capacitance, it is difficult to accurately predict coating performance based upon this data in the intermediate and high frequencies.

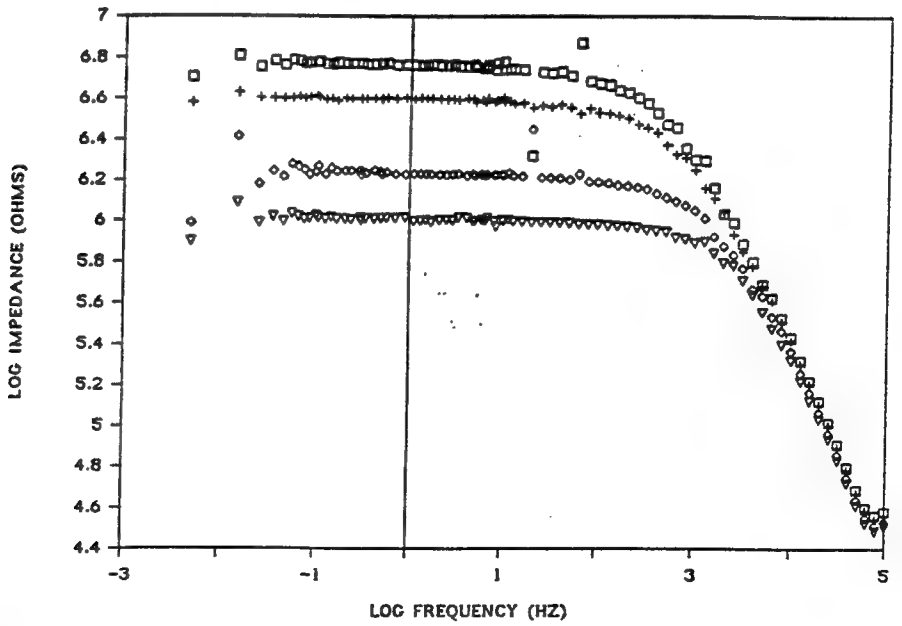

Figure 39. *Bode plot overlays of impedance spectrum from immersion testing of a coated steel sample.*

VERIFICATION OF AC IMPEDANCE RESULTS

Intentional Defect - Immersion Testing

Having established that the electrodes enable the use of the AC impedance technique, it is necessary to show that AC Impedance results do in fact represent the actual corrosion process occurring. Ellipsometry and DC potentiodynamic scans each offered a unique method for verifying the AC impedance results of scribed specimens.

To study coating degradation, an intentional defect was introduced to a lot of samples. A model of the test sample with an intentional defect is shown in Figures 40 and 41. The scribe initially penetrates through the entire oxide layer to the aluminum substrate, however, instantaneous oxide growth occurs so the aluminum substrate is never in direct contact with the electrolyte. A series of tests were performed on samples with and without conductive paint electrodes to track the water uptake, incubation, and corrosion of the aircraft coating using the AC Impedance technique. Each of the samples underwent the following tests along with visual observation each day of the testing:

1) a DC potentiodynamic scan to measure the corrosion rate,

2) an ellipsometric test to measure the refractive index, and

3) an AC Impedance test to obtain the impedance spectrum and monitor the low-frequency impedance response.

The results indicate good correlation between the three tests as seen in Figures 42 and 43. Both the waterborne epoxy primer and the epoxy polyamide primer samples display similar plots of low-frequency impedance vs time which is characteristic of the corrosion process for aircraft metal/coating systems. The act of scribing the samples drops the low-frequency impedance by four orders of magnitude. The corrosion rates of the samples jump to a peak just after the scribing has occurred. This is anticipated since the bare aluminum substrate is now exposed to the atmosphere. The corrosion rate then falls back to a lower rate as a protective oxide immediately begins to form on the exposed substrate.

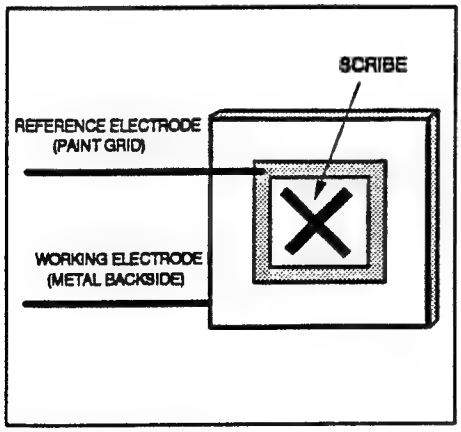

Figure 40. *Diagram of scribed sample with conductive paint electrode.*

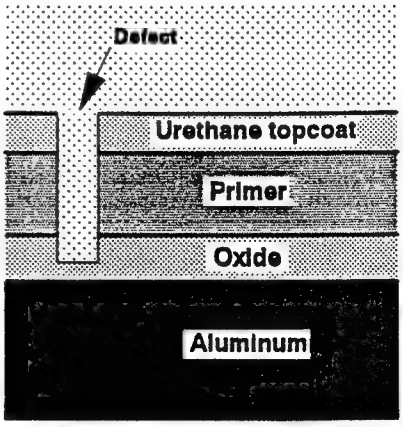

Figure 41. *Model of intentional defect in test samples.*

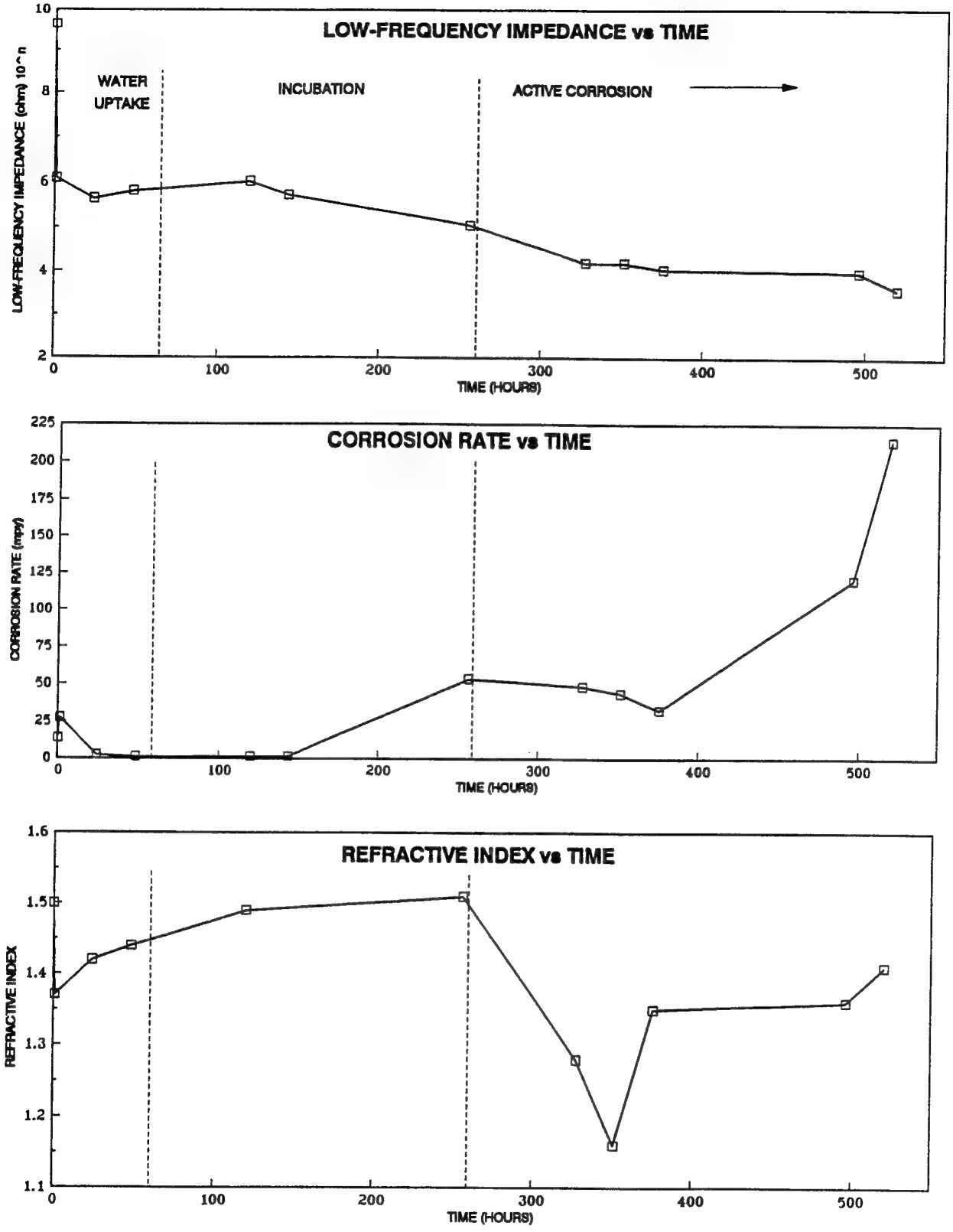

Figure 42. *Results from testing of scribed electrode-less* ***epoxy polyamide*** *Al 2024-T3 sample. To accelerate the corrosion process during the incubation stage, samples was immersed in a 5% NaCl solution for the extent of the testing.*

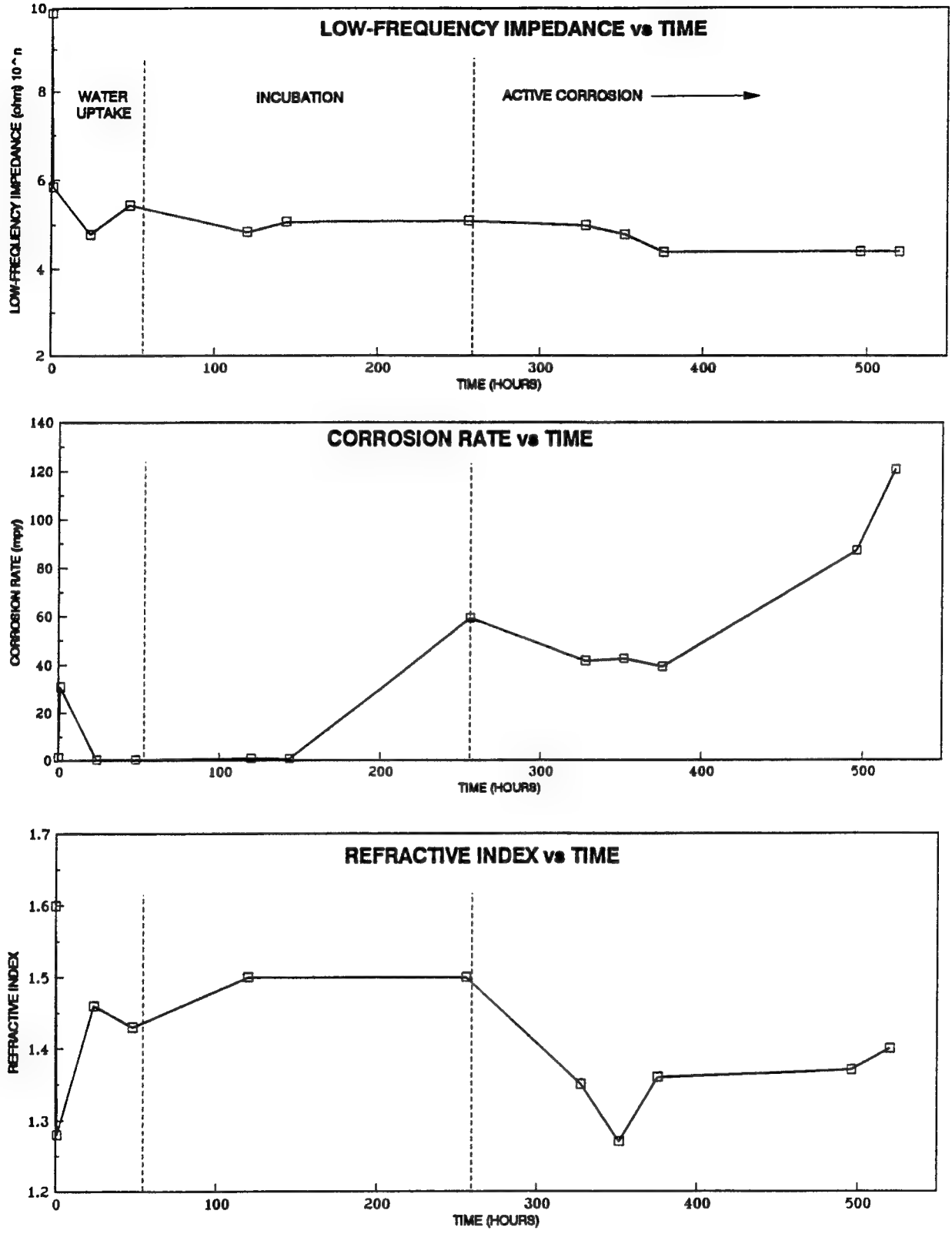

Figure 43. *Results from testing of scribed electrode-less* ***waterborne epoxy*** *Al 2024-T3 sample. To accelerate the corrosion process during the incubation stage, sample was immersed in a 5% NaCl solution for the extent of the testing.*

The results for both aircraft metal/coating systems are quite similar. Both experience the same relative corrosion process according to the plot of low-frequency impedance versus time. It is apparent that the waterborne epoxy primer is slightly more resistant to corrosion than the epoxy polyamide primer. At the onset of corrosion the epoxy polyamide experiences a sharper decline in low-frequency impedance and levels off at around 8000 ohms. The waterborne epoxy at the onset of active corrosion has a more gradual decline in low-frequency impedance and levels off at a larger low-frequency impedance of around 25000 ohms. Even though the scribe for both metal/coating systems penetrated to the substrate, the waterborne epoxy sample was able to resist corrosion more effectively. This was most likely due to the better ability of the waterborne epoxy primer to resist the ingress of water and ions into the surrounding defect area of the scribe, resulting in larger low-frequency impedance values.

The process of scribing the samples to induce corrosion bypassed the bulk of the water uptake stage of corrosion. If the samples had not been scribed, it would have been possible to monitor the water uptake of the samples until the incubation stage was reached. However, an extended amount of time is needed for the coating to absorb enough water to reach the incubation stage. Further analyses of the water uptake stage was later performed using AC Impedance in conjunction with salt fog testing.

The results from the ellipsometer indicate that definite changes occurred in the refractive index of the samples throughout the testing. The refractive index is a measure of the dispersion of the reflected light travelling through the scribed sample. The presence of the scribe damage and the resulting oxide growth has been detected. As with the impedance of the coating, the refractive index drops sharply after the scribing, indicating less dispersion of the reflected light due to the exposed aluminum substrate. The refractive index became larger again as the oxide forms. While it is difficult to directly compare the impedance and the refractive index, the plot shows that changes in the low-frequency impedance data respond well to the changes in the refractive index.

Soon after the scribing, approximately 40 hours, the samples entered the incubation period. This stage characteristically has a constant low-frequency impedance. The samples experienced an ingress of water and ions deeper into the defect and surrounding pores. This was verified by the near constant corrosion rates measured during this stage. Likewise, the refractive index slightly increased over the incubation stage as the ingress of water and ions altered the contour of the sample surface. This resulted in greater dispersion of the reflected light. Visual observation of the defect area revealed that the aluminum substrate showed no signs of discoloration or corrosion.

For the purpose of accelerating the incubation stage, the samples were placed in a 5% NaCl solution. After 250 hours of immersion, the samples began to experience active corrosion. At the onset of active corrosion, the corrosion rate increased dramatically from around 2 milli-inches (.001 in.) per year (mpy) to over 50 mpy and, correspondingly, the low-frequency impedance began to drop about 2 orders of magnitude. At this point, visual observation of the defect area revealed that the aluminum substrate had become slightly discolored and had lost some lustre. After the initial spike in the corrosion rate, the corrosion rate then leveled off at around 40 mpy before again increasing rapidly to over a 100 mpy for the waterborne epoxy and 200 mpy for the epoxy polyamide. The refractive index begins to drop at the onset of corrosion which indicates that the

corrosion has less dispersion due most likely to an initial even oxide growth. By the end of the testing, the refractive index was increasing in response to the accelerated corrosion producing uneven oxide growth. At the end of the immersion testing, the defect area was visibly corroded. The samples with the conductive paint electrode sensors showed no signs of the electrode grid de-adhering from the topcoat. The gold and carbon electrode grids showed no visual signs of degradation. The silver grid, however, had discolorations on the inside part of the grid possibly due to the ingress of the NaCl solution into the silver paint.

The results from this testing indicate thus far that low-frequency impedance is an accurate predictive means to monitor coating performance. The level of corrosion of an aircraft metal/coating system can be ascertained by a single low-frequency impedance measurement.

The use of the conductive paints to track the paint water absorption from a scribe suggests the value of further development and optimization of the electrodes. The impedance spectra of scribed two-electrode conductive paint electrode sensors as compared to scribed electrode-less samples are displayed in Figure 44. The two-electrode measurements did not indicate a drop in impedance as seen by the remote electrode of a three-electrode measurement. The three-electrode remote electrode method measures the impedance along the lowest resistivity path between the electrode and the aluminum alloy. Thus, a scribe tends to completely short-circuit the paint on the aluminum, with direct electrolyte to metal contact. The painted electrodes measure the impedance through the paint medium to the metal. As a result, a scribe contributes to a decrease in impedance only insofar as a surface conductive path exists between the conductive paint electrode across the paint to the metal. Aside from this possible contribution, it is necessary for the underlying corrosion of the metal surface to change the impedance of the paint itself by producing ionic conduction through the paint. This does not happen until the metal oxidization process dominates the formation of passive oxides. Thus, the decrease in conductive paint electrode impedance is expected to lag that of the electrode-less specimen.

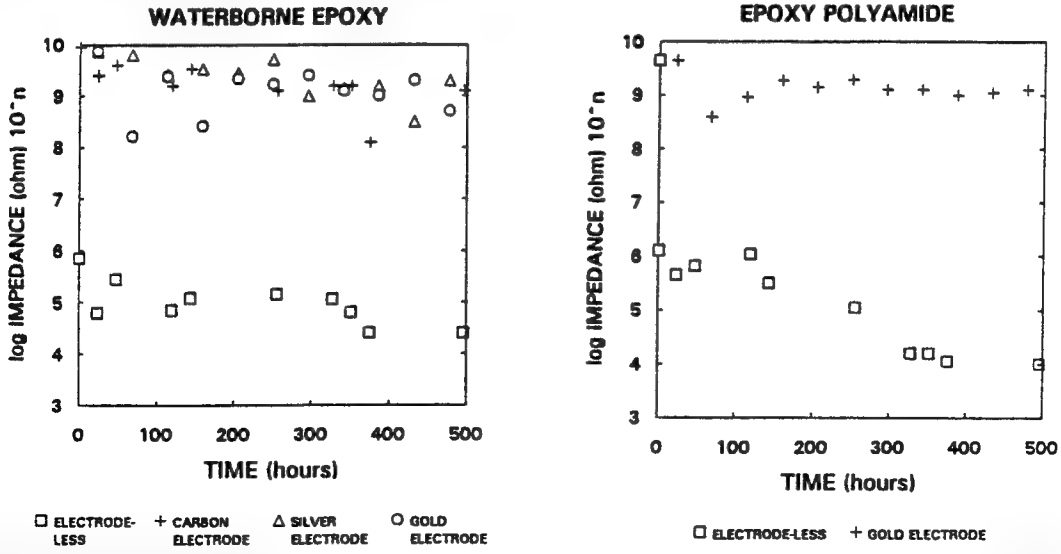

Figure 44. *Impedance spectra of conductive paint electrodes using two-electrode method and electrode-less samples using the three-electrode method.*

Salt Fog Testing

Salt spray testing was conducted in order to determine:

1) the ability of the painted electrodes to withstand harsh environments for extended exposure times,
2) the corrosion process of waterborne epoxy and epoxy polyamide primed samples without the use of a scribe, and
3) the ability of the painted electrodes to track the corrosion process.

The use of the salt spray cabinet afforded a chance to accelerate the corrosion process of the samples without the need to introduce an intentional defect. This testing enables the painted electrodes to measure the impedance of the coating more accurately than if a scribe was present. After 1020 hours of exposure, none of the electrodes (gold, silver, carbon, or nickel) showed any signs of losing integrity or de-adhering from the topcoat. In fact, the electrodes outlasted the glyptal coating applied to the backside of the samples. All samples prepared for the salt spray testing were given one heavy coat of glyptal to the metal backside and the edges of the samples. Due to the harsh environment of the salt spray, the glyptal began to peel back from the edges and blister. This exposed tiny avenues for salt spray penetration to the exposed metal backside. This resulted in corrosion products forming on the backside of the coupon and possibly creating larger impedance drops than anticipated. Testing procedure at this point was changed in order to alleviate the situation. Each sample was immediately rinsed and dried off with nitrogen and allowed to try at ambient for at least thirty minutes. This resulted in a rise in impedance values of the specimens tested after 674 hours.

The results are consistent with data obtained from the immersion testing. Impedance spectra of the remote electrode epoxy polyamide samples and the resulting low-frequency impedance vs. time corrosion curve is given in Figure 45. After about 122 hours of chamber exposure, the impedance drops about 2 orders of magnitude and, thereafter, continues a slow decrease in impedance for the remainder of the test. The resulting corrosion curve shows the initial drop (water uptake), before leveling off in the incubation period. It appears that after 674 hours of exposure, the sample did not enter the active corrosion stage. This was confirmed from visual observation, in which both the electrode and the coating appeared unchanged. Testing would have continued except for the fact that the electrode wire detached from the test specimen after 1020 hours of exposure due to penetration of the salt spray.

Salt spray results for the remote waterborne epoxy sample are shown in Figure 46. The waterborne epoxy sample displays a greater resistance to water uptake than the epoxy polyamide sample and does not drop in low-frequency impedance until 386 hours of exposure, unlike the 122 hours of exposure for the epoxy polyamide sample. These results are consistent with the immersion testing, in which, the waterborne epoxy resisted water ingress into the surrounding defect area of the coating better than the epoxy polyamide sample. After the initial water uptake, the impedance drops approximately four orders of magnitude before again increasing at 1020 hours of exposure, most likely due to the change in testing procedure. No significant decline in impedance during the incubation stage was observed, indicating that the remote sample did not enter the active corrosion region. This was supported by visual observation of the topcoat.

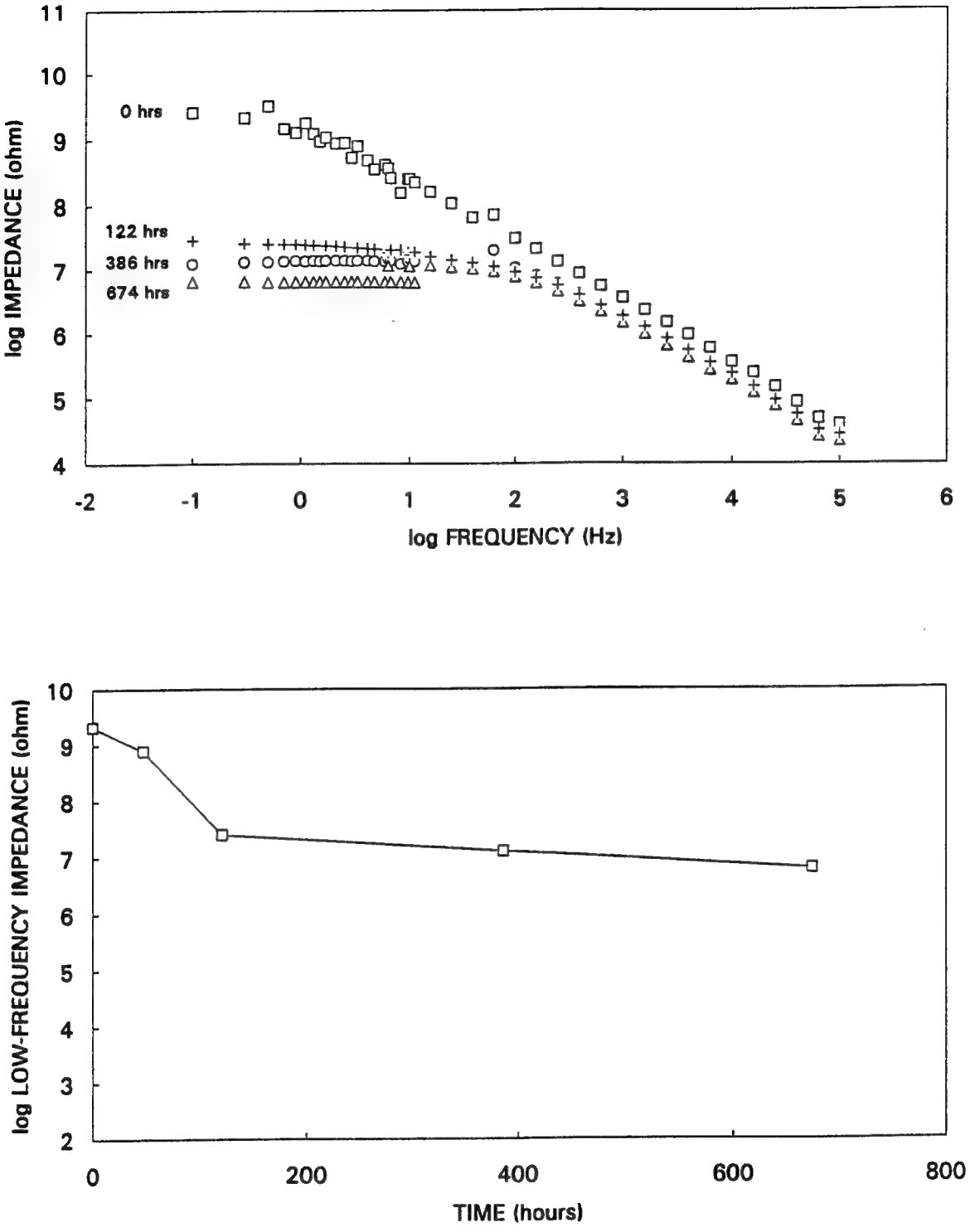

Figure 45. *AC Impedance results from salt spray testing of an aluminum 2024-T3 sample coated with epoxy polyamide primer and urethane topcoat. The top graph displays impedance spectra at various exposure times. The bottom graph shows the low-frequency impedance response (corrosion curve) to exposure time.*

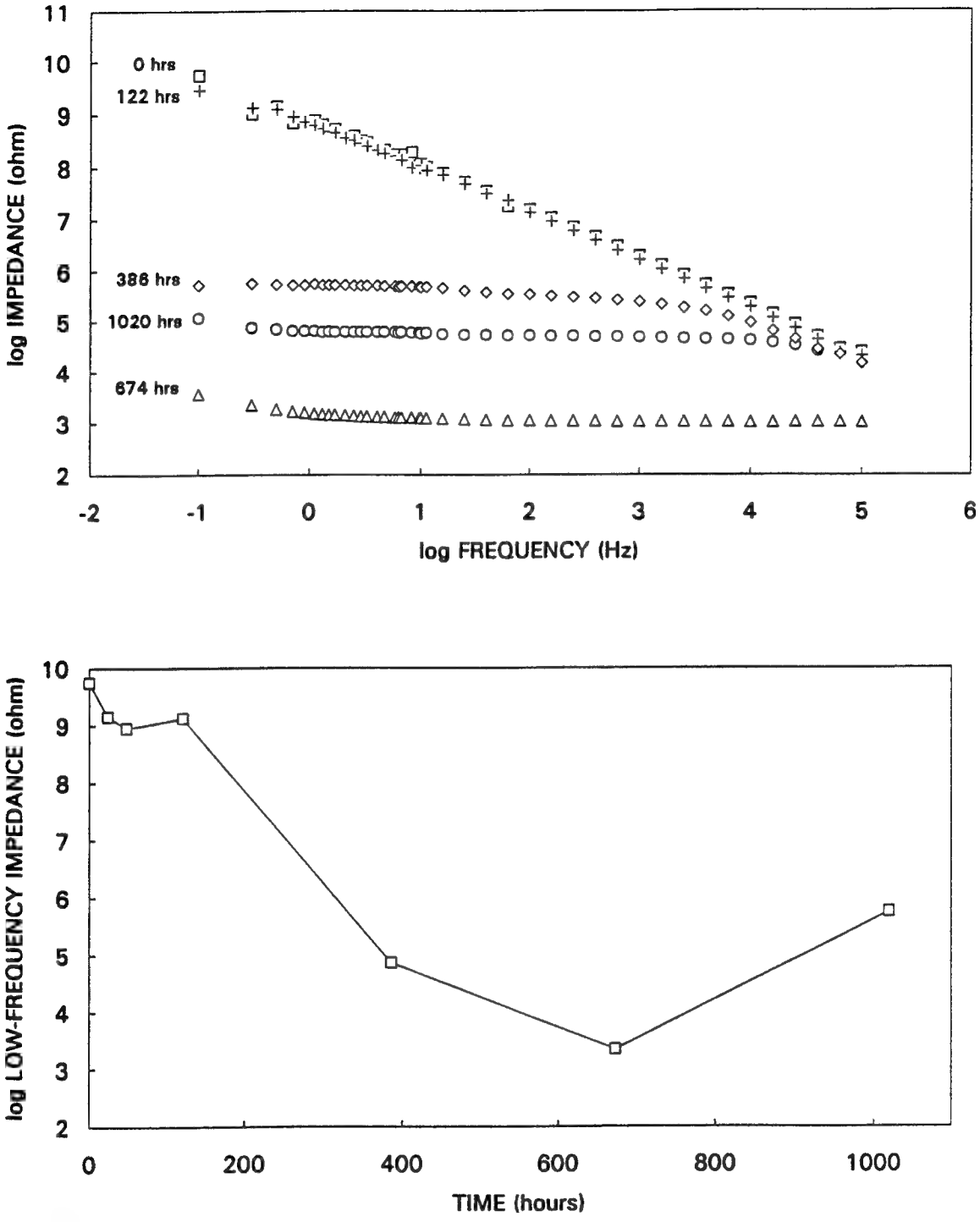

Figure 46. *AC Impedance results from salt spray testing of an aluminum 2024-T3 sample coated with* ***waterborne epoxy*** *primer and urethane topcoat. The top graph displays impedance spectra at various exposure times. The bottom graph shows the low-frequency impedance response (corrosion curve) to exposure time. The last point of the bottom graph has a higher impedance due to drying the specimen prior to the measurement.*

Figure 47 displays the AC Impedance testing results comparing the conductive paint two-electrode approach with conventional three-electrode remote testing. All the conductive paint electrodes for both primers show the ability to monitor the corrosion process, showing well-defined regions of water uptake and incubation corresponding to the conventional three-electrode results from the remote samples. The gold electrode had an excellent overlay with the remote electrode for both the waterborne and epoxy polyamide samples. The nickel, carbon, and silver electrodes have similar results, but display larger impedance values during the incubation stage than the remote. Variables such as the amount of penetration of salt spray and resulting corrosion products on the backside of coupons appear to have contributed to the differences in the overlays. Future salt spray testing will involve the samples either being coated in exactly the same manner (primer and topcoat) on all sides and edges or having several coats of glyptal applied.

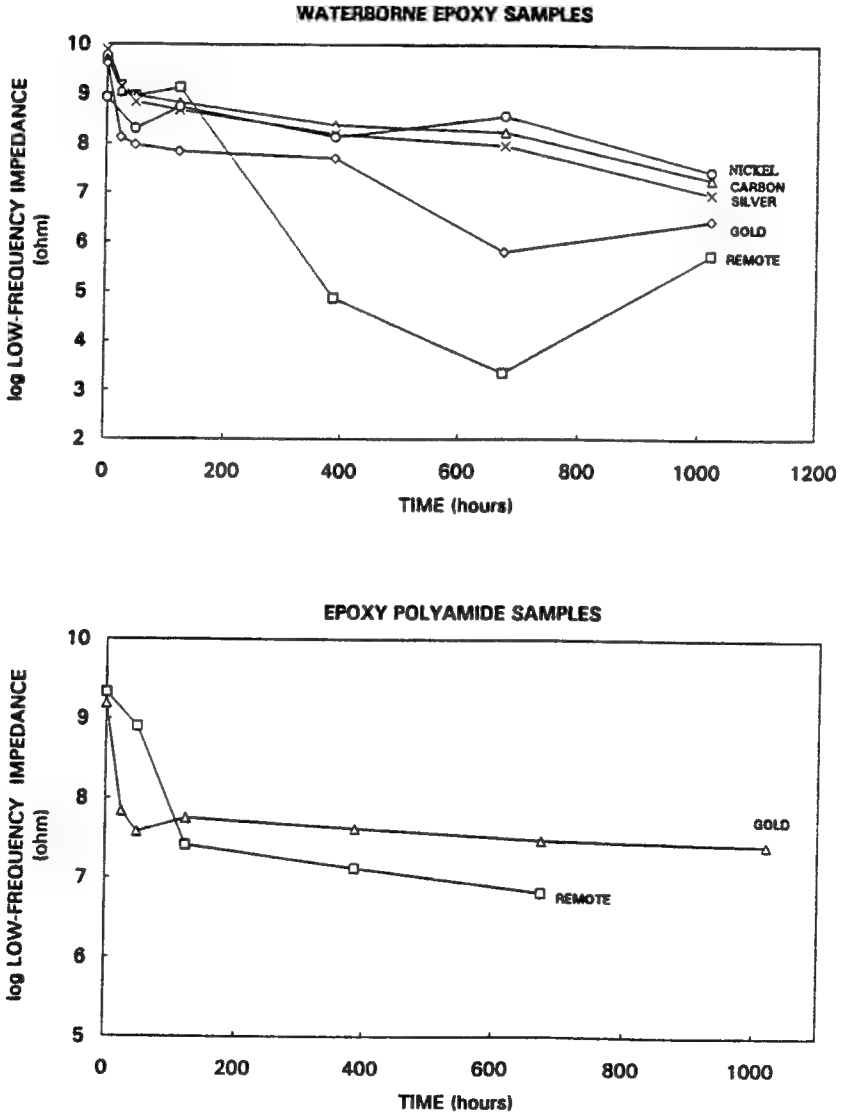

Figure 47. *Overlay AC Impedance results of two-electrode samples and conventional three-electrode remote samples from salt spray testing of aluminum 2024-T3 samples coated with epoxy polyamide primer and waterborne epoxy primer.*

As mentioned earlier, the low-frequency impedance was chosen as the parameter best suited for analyzing coating performance. The data from the salt spray testing also supports this decision. Impedance responses at various frequencies are shown in Figure 48 for both the waterborne epoxy and epoxy polyamide primers. At frequencies above 10 Hz the corrosion curve flattens out and the regions of water uptake and incubation become unclear. The lowest frequency of .3003 Hz displays the best distinction between the water uptake and incubation stages of corrosion.

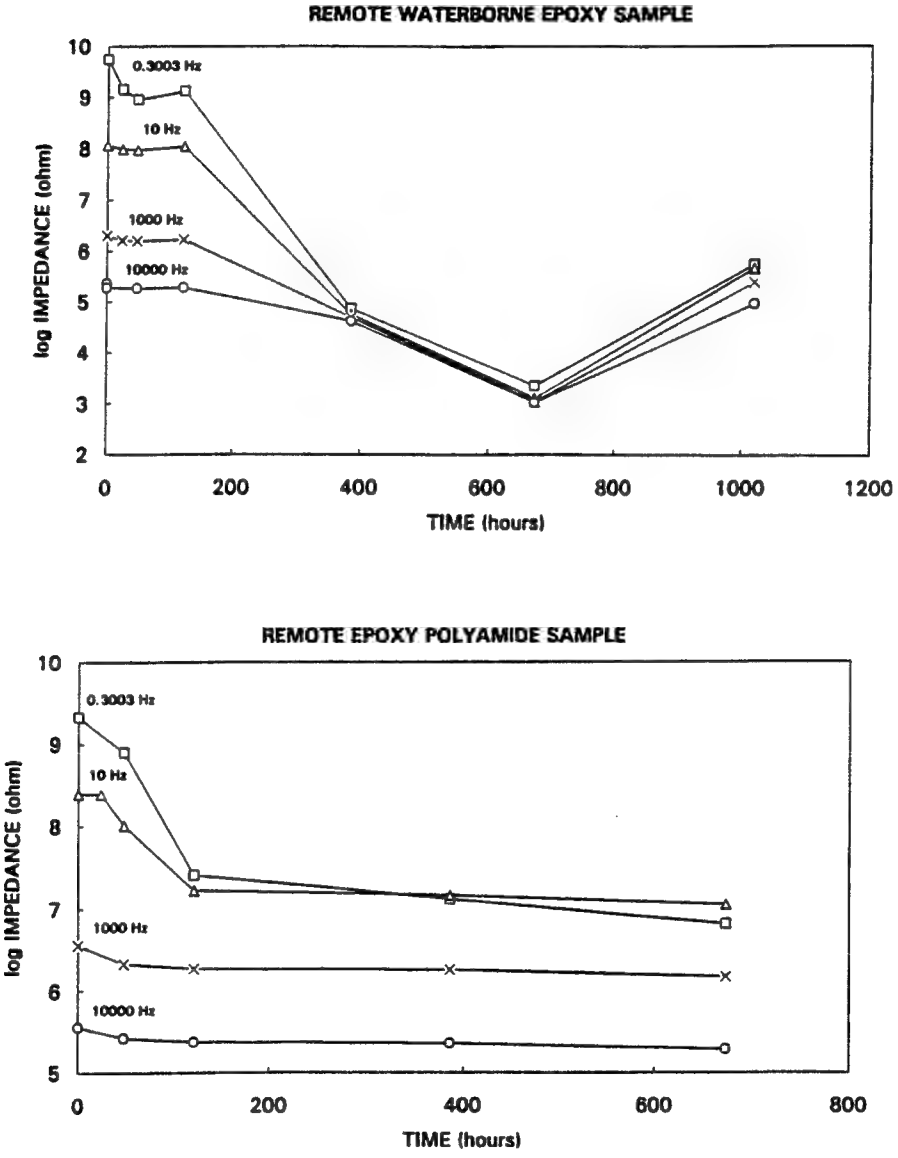

Figure 48. *Corrosion curves at various frequencies ranging from .3003 Hz to 10000 Hz. The low-frequency response of .3003 Hz generates the most predictable response displaying the best definition of water uptake and incubation.*

CONCLUSIONS:

In-situ electrode sensors capable of sensing coating degradation using the AC Impedance technique have been designed and tested. The electrode sensors have been used to generate two-electrode EIS data equivalent to data obtained using the conventional three-electrode method. Furthermore, equivalent EIS results have been obtained in aggressive environments including immersion and salt fog testing. Results from the chamber-exposed electrode sensors indicate that coating deterioration is a function of exposure time. EIS results were verified through the use of ellipsometry and DC potentiodynamic scans which correlated the amount of corrosion with near-DC low-frequency impedance values. This correlation of results indicates excellent predictive capabilities of the two-electrode sensors using the AC Impedance technique.

The research has identified and developed analytical techniques to detect coating degradation at early exposure times. These in-situ electrode sensors and their potential applicability for nondestructive, real-time analysis of coating degradation represent an opportunity to develop an uncomplicated straightforward commercial sensor which will ultimately reduce maintenance and down-time of aircraft while increasing pilot and aircraft safety.

FUTURE WORK (Phase II):

The prototype electrodes designed in the Phase I effort are capable of measuring the impedance spectra of aircraft metal/coating systems using a two-electrode approach. The design of these painted electrodes permit in-situ real-time analysis of the corrosion process by eliminating the need for both a counter electrode and the use of an electrolyte. This represents an opportunity to develop a straightforward sensor capable of quickly assessing the integrity of any metal/coating system.

Applications for these electrodes extend to all aircraft, regardless of the substrate or coating. Phase I testing included aluminum 2024-T3 coated with MIL-P-85582 waterborne epoxy and MIL-C-83286 urethane topcoat and aluminum 2024-T3 coated with MIL-P-23377 epoxy polyamide and MIL-C-83286 urethane topcoat. It was shown that a unique three-electrode impedance spectrum could be precisely obtained with electrolyte for each of these aircraft metal/coating systems. Phase I also showed that the in-situ form of our two-electrode AC Impedance sensor very closely replicated the conventional three-electrode AC Impedance results. There is no reasonable doubt that the AC Impedance technique is capable of obtaining unique impedance spectra for other metal/coating systems currently in use by the Air Force including Al 6061 and Al 7075.

Sensor design for the proposed Phase II effort includes development of both hand-held and pre-positioned in-situ sensors using the two-electrode AC Impedance technique. The hand-held sensor can then be scanned over the surface of the aircraft to pinpoint "hot spots" of corrosion present on the aircraft. The pre-positioned, in-situ sensors would be located at inaccessible areas prone to corrosion and reduce disassembly time for inspection and allow maintenance scheduling on as-needed basis. These sensors would be able to obtain the impedance spectrum from the AC excitation and be able to precisely determine what stage of corrosion (water uptake, incubation, or active corrosion) the metal/coating system is experiencing. These sensors would alert the user as to the exact status of the coating. Our proposed corrosion monitor will vastly improve an inspector's ability to detect corrosion and paint degradation in its early stages and allow prompt remedial action that could eliminate a structural failure or a costly repair.

The proposed phase II program addresses three issues: sensor electrode optimization, the packaging of the instrumentation and electronics, and establishing the effects of environmental conditions during usage. Sensor optimization will include the choice of an electrode material that will provide the maximum response and the most predictive, reproducible data. The exact range over which the electrode will be sensitive will also be established and the shape and size of the electrode will be optimized. Modification of test instrumentation packages will involve simplification of the present instrumentation and electronics along with the development of any software needed for field use.

Definition of the effect of environmental measurement conditions will establish the effective electrode range under the limitations of the environment. The limitations of severe environments will be addressed in order to develop methods to overcome these limitations. The use of ellipsometry, X-ray Photoelectron Spectroscopy, and DC electrochemical methods will correlate the Electrochemical Impedance Spectroscopy (EIS) measurements obtained for corrosion and paint de-adhesion with measured amounts of corrosion of known types.

Test instrumentation will be designed for field use. The final product will incorporate the necessary functions of a greatly simplified potentiostat, amplifier, and computer hardware and software into a single portable unit. This unit will be lightweight, rugged, and simple in design permitting the user to readily scan the aircraft to be tested. The use of simplified, integrated circuitry will increase the life of the sensor electronics and also reduce the number of repairs.

The most readily realized power of the two-electrode approach developed thus far is for incorporating the electrodes into existing aircraft or into aircraft currently being built or designed. The electrodes can be placed in any location on the aircraft whether on bare metal or a coating and do not require a large application surface area. This allows the electrodes to be placed where casual visual observation or access is not possible such as lap joints or the interior structures of wings. In addition, the electrodes can be placed at the interior surfaces of overlapping dissimilar materials subject to galvanic corrosion. Different substrate and metal/coating systems can each be evaluated according to their own unique impedance spectrum.

Further development will entail incorporating the hardware and software into the aircraft allowing for self-diagnostic scans to be run periodically. Since the present electrode of the sensor unit is only one square centimeter in size, has negligible weight, and appears to detect corrosion over a range of at least 10X its area of coverage, the presence of these electrodes is not anticipated to alter the performance or efficiency of the aircraft. In older aircraft, the electrodes can be applied when routine disassembly is required to check for corrosion. The electrodes can then be wired into a central location for periodic testing either by an inspector or by the on-board computers. In either case, this will eliminate the need for costly extended down-time of planes in order to disassemble joints and check for corrosion.

The most important benefit of this technology will be increased aircraft safety. The resulting field-operational sensor will allow maintenance inspectors to detect the early stages of corrosion of painted metal structures well before serious deterioration has occurred. Maintenance can then be scheduled based on the actual condition of the structure without visual inspection and need not be performed on an elapsed time schedule. This is particularly useful when an aircraft is subjected to either particularly harsh or benign environments, for which little accumulated evidence exists to accurately predict safe inspection and maintenance schedules. Thus, the sensor could potentially save aircraft maintenance costs in three ways: enabling inspections without costly disassembly of aircraft structures, allowing an "as-required" maintenance schedule, and initiating repairs before it becomes costly to perform them.

After the development in the proposed Phase II effort of the hand-held device and the in-situ sensor to monitor corrosion, DACCO SCI, INC. makes a commitment to have available a sum of $100,000.00 at the end of Phase II. The development of these sensors will provide tremendous follow-on opportunities. Some of the obvious opportunities would be : the manufacture and sale of the sensors, training in the use of the sensors both to the Department of Defense and to private commercial airlines, and contract services of corrosion personnel to the commercial airline industry. In addition, DACCO SCI, INC. is aggressively pursuing Non-federal follow-on Phase III funding from the commercial airlines sector, including United Airlines, McDonnell Douglas, and Lockheed.

REFERENCES:

1 Payer, J.A., Ugaiansky, G.M., "Impact of the NBS-Batelle Cost of Corrosion Study in the United States", Proc Corrosion86, Symp. Int. Approaches to Reducing Corrosion Costs (NACE, Houston, 1986).

2 Elliot, B., Chief of Structures Branch at Warners-Robbins Air Force Air Logistics Center (WR-ALC), from a talk at the 2nd Workshop on Aging Aircraft Research (Tinkers AFB, Oklahoma City, May 1994).

3 ibid.

4 Zurilla, R.W., in "Corrosion Control by Coatings" (Lehigh University, Allentown, PA, 1978).

5 Kinloch, A.J., "Adhesion and Adhesives: Science and Technology" (Chapman and Hall, London, 1987).

APPENDIX A

Certificates of Compliance
and
Epoxy and Paint Specifications

C-S Metals Service, Inc.

Aluminum
Stainless Steel

7325 WASHINGTON BOULEVARD ▫ BALTIMORE, MARYLAND 21227 ▫ (301) 796-5661

TO: ADAMS MACHINE TOOL
Box 867
COLUMBIA, MD 21044

DATE: 8/1/94

ATTN.: QUALITY ASSURANCE

Certificate of Compliance

Gentlemen:

This is to certify that the material listed below and shipped 8/1/94 on your order number VERBAL, our register number 01239 conforms to all FEDERAL specifications.

QUANTITY	MATERIAL	SIZE	SPEC.
1EA	2024 T3 T351	.032 X 36 X 48	QQA 250/4

Very truly yours, Nick Cucina

Nick Cucina
Quality Assurance Supervisor
C-S METALS SERVICE, INC.

AEROSPACE

8-10-94

Sealants, Adhesives and Coatings
1608 Fourth Street
Berkeley, CA 94710
(510) 526 1525
Fax (510) 525 5669

August 8, 1994

Chester M. Dacres Ph.D.
President
Dacco SCI, INC.
10200 Old Columbia Rd.
Columbia, MD 21040
Phone # (410) 381-9475

Dear Chester,

Enclosed please find the sixty 2" X 2" panels you requested to be coated. The panels marked with a 1, are primed with Mil-P-85582 (513X408/910X831) than topcoated with Mil-C-85285 (831K078/930K028). Panels marked with a 2, are primed with Mil-P-23377 (513X419/910X942) than topcoated with Mil-C 85285 (831K078/930K028).

If you have any other questions or concerns about the preparation of the panels, please contact me at (510) 526-1525 ext. 365.

Best Regards,

Craig Michayluk
Technical Service Representative

epoxy technology inc.

EPO-TEK® H81E

Electrically Conductive, Gold Epoxy

SPECIFICATIONS

NUMBER OF COMPONENTS ..... Two

MIXING RATIO PARTS BY VOLUME (or wt.)

Part "A" (epoxy resin & gold powder) 1

Part "B" (hardener & gold powder) 1

CURING SCHEDULE

(minimum bond line temperature)

150°C ..... 5 minutes

120°C ..... 15 minutes

80°C ..... 90 minutes

50°C ..... 12 hours

PHYSICAL PROPERTIES

Color .....Brown

Consistency . Very soft, smooth thixotropic paste

Lap Shear Strength (A1 to A1) ..... 1300 psi

Hardness, Shore A 80

Modulus of Elasticity in flexure .... 520,000 psi

Tensile Strength ..... 3,690 psi

Elongation % 0.47

Thermal Conductivity ..... 11.0 BTU in./ft²hr°F

Coefficient of Thermal Expansion 36 x 10^{-6} in/in/°C

Glass Transition Temperature — Tg —

(cured @ 150°C - 5 min.) ..... 100°C

THERMAL RESISTANCE (Junction to Case)

TO-99 package with 50 microinches of gold.

Chip size 47 x 87 mils and gold backed.

1. Eutectic Die Attach 4.2 - 4.6 °C/Watt
2. EPO-TEK H81E (2 mils thick) 7.4 - 7.8 °C/Watt

THERMAL SHOCK

Gold backed silicon chips bonded to gold metallized ceramic substrate pass: 5 cycles from –62°F to +125°F.

THERMAL CYCLING:

Gold backed silicon chips bonded to a gold metallized ceramic substrate/or metallic frame pass: 10 cycles 0°C to +150°C.

ELECTRICAL PROPERTIES

Volume Resistivity (rigid specification) 0.0004 - 0.0008 ohm-cm

PASSED MIL SPECS for salt spray, fungus resistance, acceleration and etc.

POT LIFE ..... 3 days

SHELF LIFE ..... One year at room temp. REFRIGERATION NOT REQUIRED

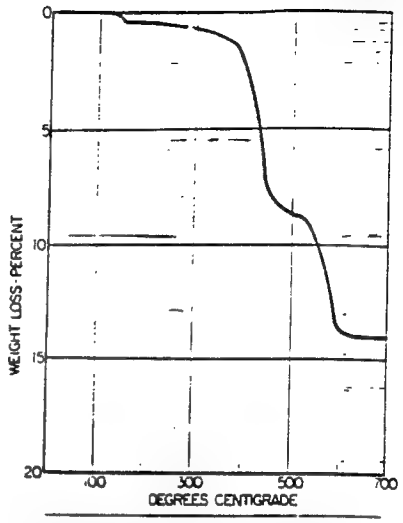

EPO-TEK H81E-
THERMAL STABILITY AS DETERMINED BY THERMOGRAVIMETRIC ANALYSIS IN AIR AT A SCAN RATE OF 20°C/MIN FROM 50°C TO 700°C

EPO-TEK H81E is a 100% solids, two component gold epoxy designed for chip bonding in microelectronic applications.

EPO-TEK H81E is a very soft, smooth thixotropic paste. The excellent handling characteristics and the long pot life at room temperature for this unique two component system is obtained without the use of solvents. In addition to the high electrical conductivity the short curing cycles and the high and proven reliability of using a pure gold powder, EPO-TEK H81E is extremely easy to use. The pure gold powder is dispersed in both the resin and hardener and the system is designed so that it can be used in a convenient 1:1 mixing ratio by volume that is non-critical. In fact EPO-TEK H81E is the easiest-to-use two component gold epoxy that has ever been developed for the microelectronics industry.

EPO-TEK H81E is especially recommended for use in high speed epoxy chip bonding systems where very fast cures are highly desirable. EPO-TEK H81E is also designed to be used in low temperature curing systems where heat sensitive devices are involved. This versatility cannot be obtained with any single component system now in existence. Because EPO-TEK H81E can be cured very rapidly, it is an excellent material to use for making fast circuit repairs.

EPO-TEK H81E is designed to be used in the 300°C to 400°C range for wire bonding operations. No refrigeration is required either in shipping or storage. Furthermore, no diluents or solvents are required at any time to adjust the viscosity of the system.

AVAILABILITY: ½ oz. trial evaluation kit, price on request, FOB Billerica, Mass. Production price schedule available on request.

EPOXY TECHNOLOGY, INC. 14 FORTUNE DRIVE, BILLERICA, MA 01821-3972 USA (508) 667-3805
1-800-227-2201 (in USA) FAX: (508) 663-9782

creative materials
incorporated

141 Middlesex Road (Rt. 3A) • Tyngsboro, MA • 01879 • (508) 649-4700 • FAX (508) 649-2040

102-05F

ELECTRICALLY CONDUCTIVE INK

DESCRIPTION: 102-05F is an electrically conductive ink, coating and adhesive suitable for screen printing very narrow circuit lines. This product features excellent adhesion to Kapton, Mylar, glass and a variety of other substrates. Unlike conventional conductive materials, this product is very resistant to abrasion and scratching. Some applications for 102-05F include, but are not limited to, emi/rfi shielding of polyimide flexible circuits, polymer thick film circuitry, membrane switches, electrical attachments for surface mounted devices, and anode coatings for tantalum capacitors. 102-05F can be further cross linked with B187 curing agent for applications requiring resistance to solvents and high humidity. Refer to handling instructions for additional information.

TYPICAL CURED PROPERTIES:

Consistency	Smooth Paste
Filler	Silver
Percent Silver (cured)	85
Crease Resistance	Excellent
Volume Resistance (ohm-cm)	0.00005
Sheet Resistivity (ohm/sq./mil)	0.019
Solderable	No
Solvent Resistance	Excellent
Hydrolytic Stability	Excellent
Useful Temperature Range	-55°C to 200°C
Thermal Stability	Good to 325°C
Coverage (wet)	28.0 in^2/gm/mil
Specific Gravity	2.52

SUGGESTED HANDLING & CURING: 102-05F is ready to use as supplied. Further thinning may be accomplished by adding small amounts of CMI Thinner #203 and/or butyl cellosolve acetate. Prior to using, be certain to resuspend silver. Best properties, for most applications, result when cured for 1 hour at 175°C. Good properties are obtained on a variety of substrates by curing at temperatures ranging from 50°C to 150°C. NOTE: Add 1phr B187 catalyst when using low temperature cures. The use of B187 is suggested to impart a high degree of chemical resistance to the conductive lines. End user is advised to experimentally determine temperature and time best suited for individual applications.

STORAGE: Shelf life: 4 months at 25°C; or 6 months at 5°C; or 12 months at -10°C.

SAFETY & HANDLING: Use with adequate ventilation. Keep away from sparks and open flames. Avoid prolonged contact with skin and breathing of vapors. Wash with soap and water to remove from skin.

Creative Materials
Incorporated

141 Middlesex Road (Rt. 3A) • Tyngsboro, MA • 01879 • (508) 649 4700 • FAX (508) 649 2040

P. WHISNANT
Sample 8/21

SAFETY DATA

REVISED: 1/28/93

IDENTIFICATION:

Product (Trade) Name: **102-05F**

General Chemical Description: SILVER FILLED POLYMER

INGREDIENTS:

Proprietary polymer and thinner: 30-40% by weight. TLV - Not Established

*Silver (CAS#7440-22-4): 60-75% by weight.
TLV: 0.1mg/m^3 (not likely to become airborne)

Gamma Amino propyl triethoxy silane (CAS#919-30-2): ~ 2% by weight.
TLV - None Established

* This material is subject to the reporting requirements of Section 313 of Title III of the Superfund Amendments and Reauthorization Act of 1986 and 40 CFR Part 372 et. seq. if present at greater than 1%.

PHYSICAL DATA:

Boiling Point (^{0}C)	> 190
Vapor Pressure @ 25^{0}C	< 2 mm Hg
Volatiles (% by weight)	> 20
Appearance and Odor	Silver paste, mild odor
Specific Gravity (water=1)	2.47-2.71
Solubility in Water	Negligible
Vapor Density	Heavier than air

FIRE AND EXPLOSION HAZARD DATA

Flashpoint: >125^{0}C
Autoignition Temp: >455^{0}C
Flammability Limits In Air (% VOL): Lower: Not Available; Upper: Not Available
Extinguishing Media: Water fog, alcohol foam, CO_2 or dry chemical extinguishing media
Special Firefighting Procedures: Firefighters should be equipped with self-contained breathing apparatus and turnout gear.
Unusual Fire and Explosive Hazards: Low, when exposed to heat or flames. Can react with oxidizing materials.

creative materials
incorporated

141 Middlesex Road (Rt. 3A) • Tyngsboro, MA • 01379 • (508) 649-4700 • FAX (508) 649-2040

104-18

ELECTRICAL RESISTOR INK

DESCRIPTION: 104-18 is an electrically resistive ink, coating and adhesive suitable for screen printing very narrow circuit lines. This product features excellent adhesion to Kapton, Mylar, glass and a variety of other substrates. Unlike conventional materials, this product is very resistant to chemicals, abrasion and scratching. Some applications for 104-18 include, but are not limited to, emi/rfi shielding of polyimide flexible circuits, polymer thick film circuitry, membrane switches, electrical attachments for surface mounted devices, and anode coatings for tantalum capacitors. 104-18 can be further cross-linked with B-187 curing agent for applications requiring resistance to solvents and high humidity. Refer to handling instructions for additional information.

TYPICAL CURED PROPERTIES:

Consistency	Smooth Paste
Filler	Carbon
Crease Resistance	Excellent
Volume Resistance (ohm-cm)	< 0.19
Sheet Resistivity (ohm/sq/mil)	< 75
Solderable	No
Solvent Resistance	Excellent
Hydrolytic Stability	Excellent
Useful Temperture Range	-55 to 200°C
Thermal Stability	Good to 325°C

SUGGESTED HANDLING & CURING: 104-18 is ready to use as supplied. Further thinning may be accomplished by adding small amounts of thinner #203 and/or butyl cellosolve acetate. Prior to using, be certain to resuspend silver. Best properties, for most applications, result when cured for 1/2 hour at 175°C. Good properties are obtained on a variety of substrates by curing at temperatures ranging from 50°C to 150°C. NOTE: Add 1phr B-187 catalyst when using low temperature cures. The use of B187 is suggested to impart a high degree of chemical resistance to the conductive lines. End user is advised to experimentally determine temperature and time best suited for individual applications.

STORAGE: Shelf life - 4 months at 25°C, or 6 months at 5°C, or 12 months at -10°C.

SAFETY & HANDLING: Use with adequate ventilation. Keep away from sparks and open flames. Avoid prolonged contact with skin and breathing of vapors. Wash with soap and water to remove from skin.

creative materials
incorporated

141 Middlesex Road (Rt. 3A) • Tyngsboro, MA • 01879 • (508) 649-4700 • FAX (508) 649-2040

SAFETY DATA

REVISED: 4/15/93

IDENTIFICATION:

Product (Trade) Name: **104-18**

General Chemical Description: Solvent-Based Epoxy Coating

INGREDIENTS:

Proprietary epoxy / curing agent / solvent mixture
No TLV established. (CMI recommends 10 ppm)

PHYSICAL DATA:

Boiling Point (°C)	>190
Vapor Pressure @ 25°C	< 2 mm Hg
Volatiles (% by weight)	<50
Appearance and Odor	Black paste, mild odor
Specific Gravity (water=1)	1.1
Solubility in Water	Negligible
Vapor Density	Heavier than air

FIRE AND EXPLOSION HAZARD DATA

Flashpoint: >125°C
Autoignition Temp: >455°C
Flammability Limits In Air (% VOL): Lower: N/A; Upper: N/A
Extinguishing Media: Water fog, alcohol foam, CO_2 or dry chemical extinguishing media
Special Firefighting Procedures: Firefighters should be equipped with self-contained breathing apparatus and turnout gear
Unusual Fire and Explosive Hazards: Low, when exposed to heat or flames. Can react with oxidizing materials.

creative materials
incorporated

141 Middlesex Road (Rt. 3A) • Tyngsboro, MA • 01879 • (508) 649-4700 • FAX (508) 649-2040

115-05

NICKEL CONDUCTIVE INK

DESCRIPTION: 115-05 is a nickel filled, conductive ink, and coating for application by screen printing, dipping and syringe dispensing. The product features excellent adhesion to Kapton, Mylar, glass and a variety of other substrates. This ink has been formulated to provide a resistance of less than 20 ohms/square/mil. when screen-printed and cure as recomended. Unlike conventional conductive materials, this product is very resistant to abrasion, scratching, flexing and creasing. Some applications for 115-05 include, but are not limited to, emi/rfi shielding of polyimide flexible circuits, polymer thick film circuitry, membrane switches and coatings for tantalum capacitors.

TYPICAL PROPERTIES:

Viscosity (cps)	18,000 - 24,000
Filler	Nickel
Crease Resistance	Excellent
Volume Resistance (Ω-cm)	0.05 max.
Sheet Resistivity (Ω/square/mil)	20 max.
Hydrolytic Stability	Excellent
Useful Temperature Range	-55°C to 200°C

SUGGESTED HANDLING & CURING: 115-05 is ready to use as supplied. Further thinning may be accomplished by adding small amounts of CMI thinner #112-18, #112-19 and/or #105-36. Prior to use, be certain to mix well to resuspend filler. **Best properties, for most applications, result when cured for 5 minutes at 110°C.** Excellent properties are also obtained on a variety of substrates by curing at temperatures ranging from 50°C to 175°C. End user is advised to experimentally determine temperature and time best suited for individual applications.

STORAGE: Shelf life: 6 months at 25°C; or 12 months at 5°C.

SAFETY & HANDLING: Use with adequate ventilation. Keep away from sparks and open flames. Avoid prolonged contact with skin and breathing of vapors. Wash with soap and water to remove from skin.

EPOXY ADHESIVES

TRA-CON TECHNICAL PRODUCT DATA

TRA-DUCT 2701

ROOM TEMPERATURE CONDUCTIVE NICKEL EPOXY ADHESIVE

DESCRIPTION

TRA-DUCT 2701 CONDUCTIVE NICKEL EPOXY ADHESIVE is an electrically-conductive nickel filled epoxy adhesive recommended for electronic bonding, sealing, and EMI/RFI shielding applications that require a combination of good electrical and mechanical properties. This two-part smooth paste formulation of pure nickel and epoxy components is free of solvents, silver, copper or carbon additives, and is in fact a low cost replacement for many silver based products. It develops strong, durable, electrically and thermally conducting coatings and bonds between many different and dissimilar materials such as metals, ceramics, glass and plastic laminates. TRA-DUCT 2701 CONDUCTIVE NICKEL EPOXY ADHESIVE cures at room temperature and can be used as a "cold-solder" for bonding and shielding heat-sensitive components, and/or in salt water exposure applications where silver-based formulations might corrode. It also can be used for the assembly and repair of electrical modules, printed circuits, wave guides, flat cable and high frequency shields.

PROPERTY	TYPICAL VALUES
Color	Nickel (grey)
Specific gravity	3.3
Viscosity, (after mixing), cps @ 25°C	Smooth paste
Mix ratio, parts by weight Hardener/Resin	6H/100R
Operating temperature range, °C	-60 to 110
Hardness, Shore D	85
Coefficient of expansion, cm/cm/°C	$49 \cdot 10^{-6}$
Thermal conductivity, cal-cm/cm² sec°C	$37 \cdot 10^{-4}$
Reactive solids content, %	100

Typical Values After Various Cure Schedules

Bond Line Cure Schedule		Volume Resistivity @ 25°C, ohm-cm	Tensile Shear alum./alum., psi
72 hours	@ 25°C	0.020	2000
1 hour	@ 65°C	0.008	—
1 hour	@110°C	0.007	—
15 minutes	@150°C	0.005	—
5 minutes	@160°C	0.003	—

APPLICATION DIRECTIONS

(1) Carefully clean and dry all surfaces to be bonded
(2) Remove clamp and thoroughly mix the TRA-DUCT 2701 CONDUCTIVE NICKEL EPOXY ADHESIVE components in the handy BIPAX® mixing-dispenser package until color is uniform throughout.
(3) Apply this completely mixed adhesive to the prepared surfaces, and gently press these surfaces together. Contact pressure is adequate for strong, reliable bonds – however maintain contact until mixed adhesive is cured.

CURE DIRECTIONS

TRA-DUCT 2701 CONDUCTIVE NICKEL EPOXY ADHESIVE has a 45 minute pot-life after thorough mixing in the accurately proportioned BIPAX® package, and a low exotherm during the cure cycle. This superior adhesive develops most of its major mechanical and structural properties after 18 hours at room temperature (overnight at 25° C), however longer cures up 72 hours at 25° C are required for fully matured bonds. The overall properties can also be attained more rapidly by curing from 2-to-4 hours at 65° C when higher cure temperatures are possible.

WARNING: THIS MATERIAL IS SOLD FOR INDUSTRIAL USE ONLY

Uncured epoxy adhesives — consisting of resin and hardener components — may cause dermatitis, skin sensitization or other allergic responses. Prevent all contact with skin and eyes. If contact occurs, flush immediately with plenty of water (get prompt medical attention for eyes). Keep away from heat and open flame. **KEEP OUT OF REACH OF CHILDREN.** Immediately clean up any spills that may occur.

TRA-CON, INC.
55 NORTH STREET, MEDFORD, MASS. 02155
PHONE (617) 391-5550 • FAX: (617) 391-7380

creative materials
incorporated

141 Middlesex Road (Rt. 3A) • Tyngsboro, MA • 01879 • (508) 649 4700 • FAX (508) 649 2040

SAFETY DATA

REVISED: 7/6/93

IDENTIFICATION:

Product (Trade) Name: **THINNER #113-12**

General Chemical Description: Solvent

Chemical Name: 2-butoxyethyl acetate

INGREDIENTS:

2-butoxyethyl acetate (CAS#000112-07-2): 95-9[illegible] % By Weight.

Gamma Amino propyl triethoxy silane (CAS#919-30-2[illegible]: < 5 % By Weight.
TLV: None Established

PHYSICAL DATA:

Boiling Point (°C)	>180
Vapor Pressure @ 20°C	< 0.5 mm Hg
Volatiles (% by weight)	>.98
Appearance and Odor	Clear liquid, no odor
Specific Gravity (water=1)	0.94
Solubility in Water	1.1%
Vapor Density	5.6

FIRE AND EXPLOSION HAZARD DATA

Flashpoint: 71°C
Autoignition Temp: 340°C
Flammability Limits In Air (% VOL): Lower: 0.88; Upper: 8.5
Extinguishing Media: Water fog, alcohol foam, CO_2 or dry chemical extinguishing media
Special Firefighting Procedures: Firefighters should be equipped with self-contained breathing apparatus and turnout gear.
Unusual Fire and Explosive Hazards: Low, when exposed to heat or flames. Can react with oxidizing materials.

Approved for public release;
distribution unlimited.